

# Disease resistance through impairment of $\alpha$ -SNAP–NSF interaction and vesicular trafficking by soybean *Rhg1*

Adam M. Bayless<sup>a</sup>, John M. Smith<sup>a</sup>, Junqi Song<sup>a,1</sup>, Patrick H. McMinn<sup>a,2</sup>, Alice Teillet<sup>a</sup>, Benjamin K. August<sup>b</sup>, and Andrew F. Bent<sup>a,3</sup>

<sup>a</sup>Department of Plant Pathology, University of Wisconsin–Madison, Madison, WI 53706; and <sup>b</sup>University of Wisconsin School of Medicine and Public Health Electron Microscopy Facility, University of Wisconsin–Madison, Madison, WI 53706

Edited by Sheng Yang He, Michigan State University, East Lansing, MI, and approved October 5, 2016 (received for review June 28, 2016)

$\alpha$ -SNAP [soluble NSF (*N*-ethylmaleimide-sensitive factor) attachment protein] and NSF proteins are conserved across eukaryotes and sustain cellular vesicle trafficking by mediating disassembly and reuse of SNARE protein complexes, which facilitate fusion of vesicles to target membranes. However, certain haplotypes of the *Rhg1* (resistance to *Heterodera glycines* 1) locus of soybean possess multiple repeat copies of an  $\alpha$ -SNAP gene (*Glyma.18G022500*) that encodes atypical amino acids at a highly conserved functional site. These *Rhg1* loci mediate resistance to soybean cyst nematode (SCN; *H. glycines*), the most economically damaging pathogen of soybeans worldwide. *Rhg1* is widely used in agriculture, but the mechanisms of *Rhg1* disease resistance have remained unclear. In the present study, we found that the resistance-type *Rhg1*  $\alpha$ -SNAP is defective in interaction with NSF. Elevated in planta expression of resistance-type *Rhg1*  $\alpha$ -SNAPs depleted the abundance of SNARE-recycling 20S complexes, disrupted vesicle trafficking, induced elevated abundance of NSF, and caused cytotoxicity. Soybean, due to ancient genome duplication events, carries other loci that encode canonical (wild-type)  $\alpha$ -SNAPs. Expression of these  $\alpha$ -SNAPs counteracted the cytotoxicity of resistance-type *Rhg1*  $\alpha$ -SNAPs. For successful growth and reproduction, SCN dramatically reprograms a set of plant root cells and must sustain this sedentary feeding site for 2–4 weeks. Immunoblots and electron microscopy immunolocalization revealed that resistance-type  $\alpha$ -SNAPs specifically hyperaccumulate relative to wild-type  $\alpha$ -SNAPs at the nematode feeding site, promoting the demise of this biotrophic interface. The paradigm of disease resistance through a dysfunctional variant of an essential gene may be applicable to other plant–pathogen interactions.

plant disease resistance |  $\alpha$ -SNAP | soybean cyst nematode | *Rhg1*

A dynamic endomembrane system is a universal trait of eukaryotic cells that enables the transfer of vesicular cargoes throughout the cell and with the cell exterior (1). Vesicle trafficking has been most deeply studied in yeast and in neuronal synapses, but is understood in detail for numerous biological systems, including immunity and host–pathogen interactions (2–5). Host and pathogen proteins can intervene to alter the course of this traffic to the benefit of the host or the pathogen (6, 7). The soybean (*Glycine max*) *Rhg1* (resistance to *Heterodera glycines* 1) locus, one of the most economically important disease resistance loci of any major food crop, carries multiple repeat copies of a gene encoding the major vesicular trafficking chaperone  $\alpha$ -SNAP [alpha-soluble NSF (*N*-ethylmaleimide-sensitive factor) attachment protein] (1, 8). The discovery that the *Rhg1*  $\alpha$ -SNAPs carry nonconsensus amino acids at widely conserved C-terminal positions of known importance was intriguing, but a mechanism by which these  $\alpha$ -SNAPs contribute to *Rhg1*-mediated soybean cyst nematode (*H. glycines*) resistance was not known (8–10).

SNARE (soluble NSF attachment protein receptor) proteins mediate vesicle fusion (1). Eukaryote genomes can encode over 100 different SNARE proteins, with various SNARE subsets generally residing at specific compartments (1). Cognate SNAREs on separate membranes promote fusion by bundling together and forming highly stable SNARE complexes that pull the respective membranes

together. SNAREs alone can mediate vesicle fusion in vitro without external energy inputs, but the *cis*-SNARE complexes formed after fusion must be separated back into free acceptor SNAREs to participate in subsequent fusion events (1).  $\alpha$ -SNAP, which is typically encoded by a single gene in animal genomes, binds diverse SNARE complexes and stimulates their disassembly by recruiting and activating NSF (1, 11). SNARE complex disassembly by  $\alpha$ -SNAP and NSF is essential for vesicular trafficking and, as such, has been studied in considerable detail. X-ray crystallography, single-molecule fluorescence spectroscopy, and cryo-EM have provided high-resolution structural insights into the dynamics of SNARE– $\alpha$ -SNAP–NSF interactions (12–14). Multiple  $\alpha$ -SNAPs stimulate disassembly of one SNARE bundle in a 20S supercomplex that includes a hexameric ring of six NSF proteins, which couple ATP hydrolysis to force-generating conformational changes.

Cyst nematodes are highly adapted obligate parasites of plant roots and cause substantial damage to world food crops, including wheat, soybean, and potato (15). Soybean cyst nematode (SCN) is responsible for the greatest yield loss in the United States of any soybean disease, and is a major constraint on soybean production worldwide (16). After penetrating the root and migrating to the root vascular bundle, SCNs secrete plant-bioactive effector proteins and other molecules through their stylet, a protrusible mouthpiece that also mediates nematode feeding on plant cells. SCN effectors collectively subdue host

## Significance

The *Rhg1* resistance locus of soybean helps control one of the most damaging diseases in world agriculture. We found that *Rhg1* (resistance to *Heterodera glycines* 1)-mediated resistance utilizes an unusual mechanism. Resistant soybeans carry a dysfunctional variant of the housekeeping protein  $\alpha$ -SNAP [soluble NSF (*N*-ethylmaleimide-sensitive factor) attachment protein]. *Rhg1* resistance-type  $\alpha$ -SNAPs interact poorly with NSF and disrupt vesicle trafficking. High levels of resistance-type  $\alpha$ -SNAPs interfere with wild-type  $\alpha$ -SNAP activities, yet are functionally balanced in most tissues by sufficient wild-type  $\alpha$ -SNAP levels. However, the biotrophic plant–pathogen interface is disabled by localized hyperaccumulation of resistance-type  $\alpha$ -SNAPs. This study suggests a paradigm of resistance conferred by a dysfunctional version of a core cellular housekeeping protein.

Author contributions: A.M.B., J.M.S., J.S., P.H.M., A.T., B.K.A., and A.F.B. designed research; A.M.B., J.M.S., J.S., P.H.M., A.T., and B.K.A. performed research; A.M.B., J.M.S., J.S., P.H.M., A.T., B.K.A., and A.F.B. analyzed data; and A.M.B., J.M.S., and A.F.B. wrote the paper.

The authors declare no conflict of interest.

This article is a PNAS Direct Submission.

<sup>1</sup>Present address: Texas A&M AgriLife Research, Department of Plant Pathology & Microbiology, Texas A&M University System, Dallas, TX 75252.

<sup>2</sup>Present address: Department of Biomedical Engineering, University of Wisconsin–Madison, Madison, WI 53706.

<sup>3</sup>To whom correspondence should be addressed. Email: afbent@wisc.edu.

This article contains supporting information online at [www.pnas.org/lookup/suppl/doi:10.1073/pnas.1610150113/-DCSupplemental](http://www.pnas.org/lookup/suppl/doi:10.1073/pnas.1610150113/-DCSupplemental).

defenses and reprogram root cells to fuse and form a metabolically hyperactive syncytium (nematode feeding site) (15, 17). Syncytium formation is a complex process involving plant cell-wall dissolution, endoreduplication, cell-cell fusion, and membrane reorganization, with the eventual incorporation of over 100 host root cells into one large multinucleate cell (15, 16, 18). Because egg-filled SCN cysts can persist in fields for many years and nematicides are often costly and environmentally damaging, the two core SCN control strategies are crop rotation to reduce inoculum load and use of SCN-resistant soybean varieties.

The soybean *Rhg1* quantitative trait locus provides the strongest known SCN resistance (19, 20). Recently, the *Rhg1* locus was molecularly isolated and characterized (8). Surprisingly, the *Rhg1* locus is a repeated block of four disparate genes that do not resemble previously known plant disease resistance mediators. Gene-silencing and gene-complementation experiments demonstrated contributions to SCN resistance for three of the four tightly linked genes on the *Rhg1* repeat: *Glyma.18G022400* (encoding a putative amino acid permease, formerly *Glyma18g02580*), *Glyma.18G022500* (encoding a predicted  $\alpha$ -SNAP, formerly *Glyma18g02590*), and *Glyma.18G022700* (a predicted wound-inducible protein, formerly *Glyma18g02610*) (8). Expressing any of the single genes found within the repeated *Rhg1* block, including the resistance-associated *Rhg1*  $\alpha$ -SNAP, did not detectably elevate SCN resistance, but simultaneous expression of the resistance-associated *Rhg1*  $\alpha$ -SNAP with the other genes encoded within the *Rhg1* ~31-kb repeat segment enhanced SCN resistance (8). The ~31-kb *Rhg1* segment is present in a single copy in SCN-susceptible soybean varieties, but multiple direct repeat copies are present in SCN-resistant varieties (8). Two distinct classes of resistance-encoding *Rhg1* haplotypes have been identified: low-copy (three copies or fewer) and high-copy (more than four copies); the low- and high-copy *Rhg1* haplotypes each encode distinct polymorphic  $\alpha$ -SNAPs (Fig. 1A) (9, 21). No amino acid polymorphisms are predicted in the *Glyma.18G022400* or *Glyma.18G022700* products from SCN-susceptible as opposed to SCN-resistant *Rhg1* haplotypes, but *Rhg1* copy-number expansion constitutively elevates the transcript levels of these genes in SCN-resistant plants (9). The polymorphisms in the *Rhg1* *Glyma.18G022500*-encoded  $\alpha$ -SNAP are at the highly conserved C terminus, which in mammal and yeast systems directly contacts NSF and is required for activation of SNARE disassembly (8–10, 14).

For over 30 y the soybean industry has relied on extensive use of *Rhg1* from a single source, PI 88788 (22). Field SCN populations evolve slowly, but are increasingly exhibiting partial virulence on plants expressing PI 88788-derived *Rhg1* (23, 24). Understanding the molecular mechanisms of *Rhg1*-mediated SCN resistance may allow quantitative improvements to *Rhg1* resistance through allele diversification, the generation of synthetic improved resistance, and/or transfer of the widely successful *Rhg1*-mediated resistance mechanism to other crops, such as wheat or potato. In this study, we used in vitro and in planta methods to functionally characterize *Rhg1*-encoded  $\alpha$ -SNAPs. We discovered the unusual presence of a stably inherited  $\alpha$ -SNAP that is toxic to normal  $\alpha$ -SNAP-NSF interactions and vesicular trafficking yet is beneficial during the *Rhg1*-mediated SCN resistance response of soybean.

## Results

***Rhg1* Resistance-Type  $\alpha$ -SNAPs That Are Polymorphic at Conserved Residues Are Impaired in NSF Interactions.** The C-terminal six amino acid residues of  $\alpha$ -SNAPs are very highly conserved across eukaryotes, with three or four acidic residues followed by the near-universal penultimate leucine (Fig. S1A). Most soybeans are susceptible to SCN, and their single-copy *Rhg1* locus  $\alpha$ -SNAP matches this consensus, but the SCN resistance-conferring high-copy or low-copy *Rhg1* loci encode multiple copies of  $\alpha$ -SNAPs that diverge at these sites and an upstream residue (Fig. 1A) (9, 21). Because electrostatic contacts between the NSF N domain

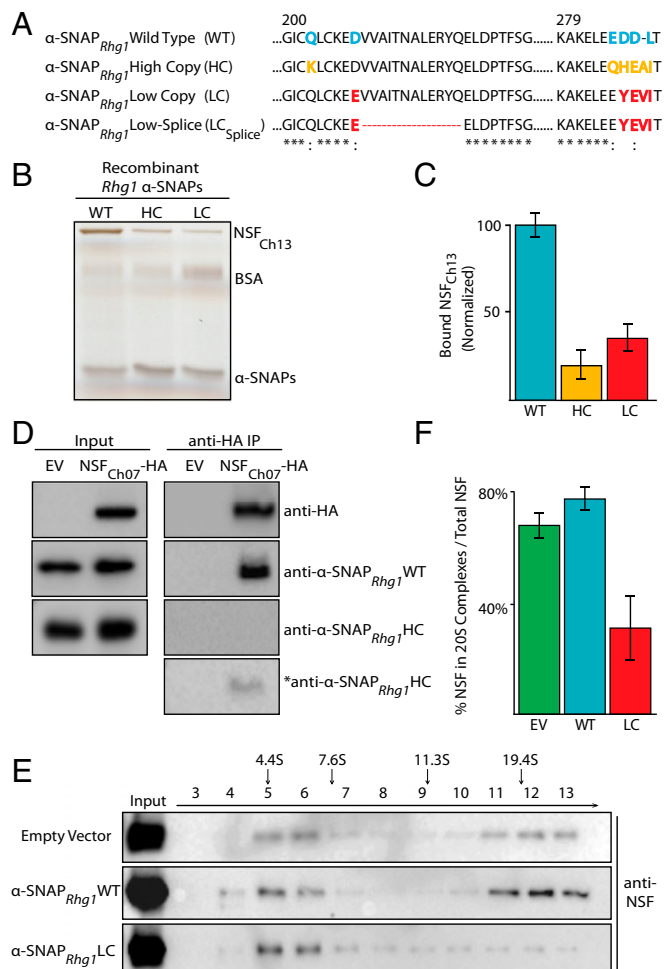


**Fig. 1.** *Rhg1* resistance-type  $\alpha$ -SNAPs are deficient in NSF interactions and destabilize 20S complexes. (A) Alignment of *Rhg1* single-copy (wild-type, SCN-susceptible), low-copy (SCN-resistant), and high-copy (SCN-resistant)  $\alpha$ -SNAPs (9), showing resistance-type amino acid polymorphisms, and an alternate splice form of the low-copy  $\alpha$ -SNAP. Asterisks indicate identical amino acid residues; colons indicate similar residues. (B) Silver-stained SDS/PAGE of recombinant soybean NSF<sub>Ch13</sub> bound in vitro by recombinant wild-type, low-copy (LC), or high-copy (HC) *Rhg1*  $\alpha$ -SNAP proteins. BSA, bovine serum albumin. (C) Densitometric quantification of NSF<sub>Ch13</sub> bound by *Rhg1*  $\alpha$ -SNAPs as in B; data are from three independent NSF<sub>Ch13</sub> experiments. Error bars show SEM. (D) Immunoblot of coimmunoprecipitation of endogenous WT  $\alpha$ -SNAP and  $\alpha$ -SNAP<sub>*Rhg1*</sub>HC upon anti-HA immunoprecipitation (IP) of soybean NSF<sub>Ch07</sub>-HA in transgenic Fayette roots.  $\alpha$ -SNAP detection was with custom antibodies (Fig. S2 A–C). Input: total protein samples before immunoprecipitation. EV, empty vector. All panels were exposed for 20 s, except for an 8-min exposure for final panel, labeled with an asterisk. (E) Immunoblot of density gradient fractions to detect the presence of NSF in 20S complexes. Total solubilized membrane proteins were loaded from *N. benthamiana* leaves expressing either  $\alpha$ -SNAP<sub>*Rhg1*</sub>LC,  $\alpha$ -SNAP<sub>*Rhg1*</sub>WT, or empty vector, and anti-NSF antibody was used to detect endogenous *N. benthamiana* NSF after SDS/PAGE immunoblotting of the resulting fractions. (F) Quantification of NSF present in 20S complexes. Densitometric data are from four independent experiments, calculated as the combined density of NSF signal in ~20S-migrating fractions (fractions 11 to 13) over the total NSF density (fractions 3 to 13). Error bars show SEM.

and the acidic residues at the  $\alpha$ -SNAP C terminus are reported in animal systems (12), we examined NSF binding by *Rhg1*  $\alpha$ -SNAPs. The reference Williams 82 soybean genome encodes two NSF proteins, *Glyma.07G195900* (NSF<sub>Ch07</sub>) and *Glyma.13G180100* (NSF<sub>Ch13</sub>), which are 98% identical. For in vitro binding studies, we generated recombinant NSF<sub>Ch07</sub> and NSF<sub>Ch13</sub> proteins as well as recombinant *Rhg1*  $\alpha$ -SNAP proteins of the high-copy type (PI 88788-type) and low-copy type (Peking-type), designated  $\alpha$ -SNAP<sub>*Rhg1*</sub>HC

and  $\alpha$ -SNAP<sup>Rhg1</sup>LC, respectively, and the SCN-susceptible Williams 82 wild-type  $\alpha$ -SNAP ( $\alpha$ -SNAP<sup>Rhg1</sup>WT). In vitro NSF binding assays were performed essentially as in ref. 25. We observed that NSF<sup>Ch07</sup> or NSF<sup>Ch13</sup> binding to either  $\alpha$ -SNAP<sup>Rhg1</sup>HC or  $\alpha$ -SNAP<sup>Rhg1</sup>LC was reduced  $\sim$ 60 to 70% compared with  $\alpha$ -SNAP<sup>Rhg1</sup>WT (Fig. 1 B and C and Fig. S1 B and C). In soybean, we have detected an alternatively spliced transcript for the low-copy  $\alpha$ -SNAP ( $\alpha$ -SNAP<sup>Rhg1</sup>LC<sub>Splice</sub>), representing  $\sim$ 20% of total  $\alpha$ -SNAP<sup>Rhg1</sup>LC transcripts (Fig. S1D) (9). The  $\alpha$ -SNAP encoded by the  $\alpha$ -SNAP<sup>Rhg1</sup>LC<sub>Splice</sub> transcript, which retains the same C terminus but removes residues 209 to 221 (Fig. 1A), also bound NSF poorly (Fig. S1E). The requirement of the soybean  $\alpha$ -SNAP C terminus for NSF binding was examined by truncating the final 10 C-terminal residues of  $\alpha$ -SNAP<sup>Rhg1</sup>WT [ $\alpha$ -SNAP<sup>Rhg1</sup>WT(-10)]; little to no binding of NSF<sup>Ch07</sup> by this protein was observed (Fig. S1E). We examined the conservation of the  $\alpha$ -SNAP C terminus in NSF binding across distant eukaryotes by testing the binding of Chinese hamster NSF (NSF<sup>CHO</sup>; 45% identity to soybean NSF) with soybean *Rhg1*  $\alpha$ -SNAPs. Robust binding of NSF<sup>CHO</sup> to  $\alpha$ -SNAP<sup>Rhg1</sup>WT was observed, whereas NSF<sup>CHO</sup> binding to either  $\alpha$ -SNAP<sup>Rhg1</sup>HC or  $\alpha$ -SNAP<sup>Rhg1</sup>LC was reduced  $>$ 80%, indicating strong conservation of the  $\alpha$ -SNAP C terminus for NSF interactions (Fig. S1 F and G).

Free, unbound  $\alpha$ -SNAP is not reported to establish NSF binding interfaces; rather, NSF is recruited by  $\alpha$ -SNAPs bound to SNAREs or immobilized on a plastic surface (1, 25). To confirm reduced NSF interactions with the *Rhg1* resistance-type  $\alpha$ -SNAPs in planta, we performed coimmunoprecipitation (co-IP) assays in transgenic roots of soybean variety Fayette (high-copy *Rhg1*) expressing NSF<sup>Ch07</sup>-HA. Similar to our in vitro studies, we observed reduced interaction between NSF<sup>Ch07</sup>-HA and endogenous  $\alpha$ -SNAP<sup>Rhg1</sup>HC compared with endogenous WT  $\alpha$ -SNAPs (Fig. 1D). Detection of WT  $\alpha$ -SNAP or  $\alpha$ -SNAP<sup>Rhg1</sup>HC was performed using custom antibodies raised against native peptides mapping to the extreme  $\alpha$ -SNAP C terminus (see Fig. S2 A–C for custom antibody specificity). When expressing soybean NSF<sup>Ch07</sup>-HA and GFP- $\alpha$ -SNAP<sup>Rhg1</sup>HC or GFP- $\alpha$ -SNAP<sup>Rhg1</sup>WT in *Nicotiana benthamiana* leaves via agroinfiltration, we again reproducibly detected substantial decreases in NSF binding to  $\alpha$ -SNAP<sup>Rhg1</sup>HC compared with  $\alpha$ -SNAP<sup>Rhg1</sup>WT (Fig. S1H).

*cis*-SNARE complexes formed from vesicle fusion events are recycled in a 20S supercomplex of multiple  $\alpha$ -SNAPs interfaced with the NSF hexamer (1, 12). We examined whether 20S complex levels in *N. benthamiana* were affected by  $\alpha$ -SNAP<sup>Rhg1</sup>LC expression. Glycerol gradient ultracentrifugation and fractionation of detergent-solubilized membrane proteins determined that  $\alpha$ -SNAP<sup>Rhg1</sup>LC decreased the amount of endogenous membrane-associated NSF in 20S fractions by  $>$ 50% (Fig. 1 E and F). A greater proportion of NSF was detected in fractions sedimenting below 20S, suggesting 20S complex instability. On the other hand, with  $\alpha$ -SNAP<sup>Rhg1</sup>WT expression, the majority of total membrane-associated NSF remained in 20S-sedimenting fractions, similar to empty vector controls (Fig. 1E). Fraction identity was confirmed with parallel cofractionation of protein standards of known sedimentation (Fig. S3). The specificity of custom antibodies raised against NSF-based peptides was confirmed (Fig. S2D). Because multiple  $\alpha$ -SNAPs participate in stimulating SNARE disassembly by NSF in the 20S complex, 20S destabilization is likely to mean fewer and potentially less productive interactions between wild-type  $\alpha$ -SNAPs and NSF. Together, our in vitro and in planta results suggest that SCN resistance-conferring  $\alpha$ -SNAPs are compromised in promoting NSF function.

**Resistance-Type  $\alpha$ -SNAPs Are Cytotoxic at High Doses and Trigger Elevated NSF Abundance.** We observed that expressing either resistance-type *Rhg1*  $\alpha$ -SNAP ( $\alpha$ -SNAP<sup>Rhg1</sup>LC or  $\alpha$ -SNAP<sup>Rhg1</sup>HC) in *N. benthamiana* caused visible chlorosis 3 to 4 d after agroinfiltration, with extensive cell death occurring 1 to 3 d later (Fig. 2A). Cell death induced by  $\alpha$ -SNAP<sup>Rhg1</sup>LC was consistently

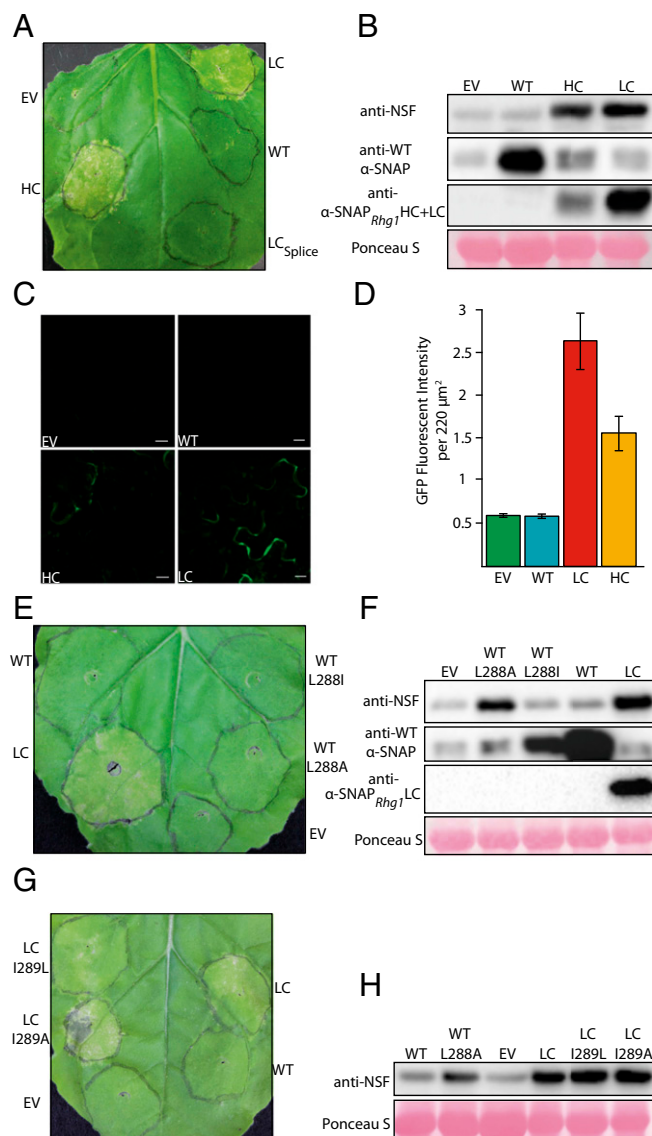


**Fig. 2.** *Rhg1* resistance-type  $\alpha$ -SNAP expression disrupts secretory trafficking, triggers NSF hyperaccumulation, and eventually causes cell death in *N. benthamiana*. (A) *N. benthamiana* leaf expressing *Rhg1*  $\alpha$ -SNAPs with no epitope tag, or an empty vector control, 6 d after agroinfiltration. HC,  $\alpha$ -SNAP<sup>Rhg1</sup>HC; LC,  $\alpha$ -SNAP<sup>Rhg1</sup>LC; LC<sub>Splice</sub>,  $\alpha$ -SNAP<sup>Rhg1</sup>LC<sub>Splice</sub>; WT,  $\alpha$ -SNAP<sup>Rhg1</sup>WT. (B) Immunoblot of endogenous *N. benthamiana* NSF abundance in leaves expressing the indicated  $\alpha$ -SNAP<sup>Rhg1</sup> constructs from A or empty vector control. The same samples were probed with anti- $\alpha$ -SNAP<sup>Rhg1</sup> antibodies raised against peptides from the indicated source. Leaf tissue was harvested 3 d after agroinfiltration; Ponceau S staining shows similar loading of total protein. (C) Confocal images of *N. benthamiana* epidermal cells coexpressing sec-GFP and *Rhg1*-encoded  $\alpha$ -SNAPs denoted as in A, or empty vector control. The sec-GFP assay detects GFP signal if there is failed secretion (retention in ER–Golgi). Images are for 3 d after agroinfiltration. (Scale bars, 20  $\mu$ m.) (D) Quantification of sec-GFP fluorescence with the respective *Rhg1*-encoded  $\alpha$ -SNAPs as shown in C using ImageJ;  $n = 25$  for each construct. Error bars show SEM. (E and G) *N. benthamiana* leaves 5 d after agroinfiltration to express the indicated *Rhg1*  $\alpha$ -SNAPs with no epitope tag, *Rhg1*  $\alpha$ -SNAPs mutagenized to carry different residues at the penultimate amino acid (no epitope tag), or an empty vector control. (F and H) Endogenous *N. benthamiana* NSF abundance at 3 d as in B, upon expression of the indicated  $\alpha$ -SNAP<sup>Rhg1</sup> constructs from E or G, respectively, or empty vector control.

observed to occur 1 to 2 d earlier than from  $\alpha$ -SNAP<sup>Rhg1</sup>HC. Expressing  $\alpha$ -SNAP<sup>Rhg1</sup>WT or  $\alpha$ -SNAP<sup>Rhg1</sup>LC<sub>Splice</sub> did not result

in cell death or other macroscopic phenotypes indicative of stress (Fig. 2A). Expression of  $\alpha$ -SNAP<sup>Rhg1</sup>WT or either resistance-type  $\alpha$ -SNAP was confirmed using custom antibodies (Fig. 2B and Fig. S2 A–C). The  $\alpha$ -SNAP<sup>Rhg1</sup>LC<sup>Splice</sup> protein was not observed to accumulate in *N. benthamiana* or in transgenic soybean roots (Fig. S4). Cytotoxicity of resistance-type  $\alpha$ -SNAP was also observed, but with a delayed onset, when the proteins were expressed in *N. benthamiana* from the native *Rhg1* promoter in the presence of the other *Rhg1* repeat-associated genes (Fig. S5A). Serial twofold dilutions of  $\alpha$ -SNAP<sup>Rhg1</sup>LC delivery confirmed dose sensitivity of the observed cytotoxicity (Fig. S5B).

To test the hypothesis that the cytotoxicity of the unusual resistance-type  $\alpha$ -SNAPs may be due to disruption of NSF-dependent processes, we tested whether a defective NSF would recapitulate this cytotoxicity. Mutagenizing a conserved glutamate in the NSF D1 domain Walker B motif generates a dominant-negative ATPase-null NSF (26). We assessed the impact of directly blocking NSF ATPase in *N. benthamiana* by generating the analogous mutation in soybean NSF (NSF<sup>Ch07</sup>E332Q). Expressing NSF<sup>Ch07</sup>E332Q caused a cytotoxic symptom onset and severity similar to  $\alpha$ -SNAP<sup>Rhg1</sup>LC expression, whereas expression of wild-type NSF<sup>Ch07</sup> had no effect, similar to empty vector controls (Fig. S6).

A strong increase in abundance of the endogenous *N. benthamiana* NSF protein was consistently detected in leaves expressing cytotoxic  $\alpha$ -SNAPs, whereas expression of  $\alpha$ -SNAP<sup>Rhg1</sup>WT did not affect NSF levels (Fig. 2B; see also Fig. 2 F and H). To determine whether elevated NSF expression was specific to resistance-type  $\alpha$ -SNAP expression or a hallmark of stressed cells, we treated leaves with the herbicide paraquat (50  $\mu$ M) for 24 h and did not observe significant changes in NSF expression (Fig. S7A). No significant changes in NSF expression were observed in transgenic soybean roots expressing resistance-type  $\alpha$ -SNAPs (Fig. S7 B and C). Nonetheless, modulation of NSF protein levels from disrupting  $\alpha$ -SNAP function is apparently unreported in other systems, and may be a feedback mechanism characteristic to some plants (27–29).

**Resistance-Type  $\alpha$ -SNAPs Disrupt Secretion and *trans*-Golgi Network Trafficking.** Regeneration of free acceptor SNAREs via *cis*-SNARE complex disassembly is necessary for ongoing vesicle trafficking. Because resistance-type  $\alpha$ -SNAPs interacted poorly with NSF, we assessed their impacts on exocytic trafficking in *N. benthamiana* using the sec-GFP secreted GFP assay (30). In this assay, if the engineered sec-GFP protein is secreted extracellularly from the endoplasmic reticulum (ER) to the apoplast, it fluoresces weakly, but if trafficking is disrupted and sec-GFP is retained in the ER–Golgi network, it fluoresces strongly (30). Samples were monitored at 2 and 3 d after agroinfiltration, before the onset of chlorotic leaf symptoms. Resistance-type  $\alpha$ -SNAP coexpression with sec-GFP strongly induced intracellular sec-GFP fluorescence, whereas  $\alpha$ -SNAP<sup>Rhg1</sup>WT resembled empty vector controls and did not perturb sec-GFP trafficking, as evidenced by a lack of fluorescence accumulation (Fig. 2 C and D). We additionally examined whether resistance-type  $\alpha$ -SNAPs affect Golgi network trafficking using the *trans*-Golgi network/early endosome marker SYNTAXIN OF PLANTS 61 (Syp61)-mCherry (31). In the vast majority of cells, coexpression of  $\alpha$ -SNAP<sup>Rhg1</sup>WT did not substantially alter the punctate vesicle and plasma membrane distribution and abundance of Syp61 fluorescence seen in empty vector controls.  $\alpha$ -SNAP<sup>Rhg1</sup>LC expression, however, shifted the Syp61-mCherry signal to an extensive and diffuse distribution (albeit excluded from chloroplasts, nuclei, and vacuoles) (Fig. S8). The sec-GFP and Syp61-mCherry results indicate that high expression of resistance-type  $\alpha$ -SNAPs disrupts exocytosis and normal trafficking through the Golgi.

**Substituting the Penultimate Leucine Modulates Cell-Death Progression from Resistance-Type  $\alpha$ -SNAPs.** The penultimate leucine is seemingly conserved across all other available plant and animal  $\alpha$ -SNAP sequences, yet resistance-type soybean *Rhg1*  $\alpha$ -SNAPs have an

isoleucine at this position (Fig. S14) (10). In vitro studies of yeast and animal NSF have demonstrated that this leucine enhances NSF ATPase activity, and that  $\alpha$ -SNAP with an engineered leucine-to-alanine substitution at this position no longer stimulates ATPase activity or SNARE disassembly (10, 14). We therefore assessed the effects of penultimate leucine substitutions in *Rhg1*  $\alpha$ -SNAPs. Curiously, no cytotoxic symptoms in *N. benthamiana* were apparent from  $\alpha$ -SNAP<sup>Rhg1</sup>WT-L288A or  $\alpha$ -SNAP<sup>Rhg1</sup>WT-L288I (Fig. 2E). However, we detected that NSF protein levels were substantially elevated by  $\alpha$ -SNAP<sup>Rhg1</sup>WT-L288A and not by  $\alpha$ -SNAP<sup>Rhg1</sup>WT or  $\alpha$ -SNAP<sup>Rhg1</sup>WT-L288I, further suggesting that elevation of endogenous NSF is due to dysfunctional  $\alpha$ -SNAPs and not cell death (Fig. 2F). In an otherwise wild-type  $\alpha$ -SNAP, absence of the penultimate leucine is sufficient to trigger increases in NSF protein abundance, but not cell death.

In contrast to results with the wild-type  $\alpha$ -SNAP, in  $\alpha$ -SNAP<sup>Rhg1</sup>LC (Fig. 1A), alanine substitution ( $\alpha$ -SNAP<sup>Rhg1</sup>LC-I289A) did enhance the progression of chlorosis and cytotoxicity (Fig. 2G). Conversely, placing a penultimate leucine in a resistance-type  $\alpha$ -SNAP ( $\alpha$ -SNAP<sup>Rhg1</sup>LC-I289L) modestly reduced toxicity progression compared with unaltered  $\alpha$ -SNAP<sup>Rhg1</sup>LC (Fig. 2G). All  $\alpha$ -SNAP<sup>Rhg1</sup>LC substitutions eventually resulted in chlorosis and cell death, with large increases in NSF production (Fig. 2H). Similar results were observed with  $\alpha$ -SNAP<sup>Rhg1</sup>HC penultimate substitutions (Fig. S9A). Expressing the C-terminally truncated  $\alpha$ -SNAP<sup>Rhg1</sup>WT(-10), which did not strongly bind NSF in vitro, elicited strong cytotoxic effects, similar to resistance-type  $\alpha$ -SNAPs (Fig. S9B). Overall, these results indicate that substitution of the penultimate leucine for isoleucine contributes to the in planta cytotoxicity of resistance-type *Rhg1*  $\alpha$ -SNAPs but that the other C-terminal residue changes also contribute to the full effect. The results further indicate that the presence of a penultimate isoleucine, compared with a more extreme change (such as leucine-to-alanine), apparently mutes the severity of the resistance-type *Rhg1*  $\alpha$ -SNAP alleles.

**Wild-Type Soybean  $\alpha$ -SNAPs Alleviate the Cytotoxicity and Secretion Defects of Resistance-Type  $\alpha$ -SNAPs.** Due largely to two ancient genome polyploidization/duplication events (32), the Williams 82 soybean genome encodes five different  $\alpha$ -SNAPs: *Glyma.02G260400*, *Glyma.09G279400*, *Glyma.11G234500*, *Glyma.14G054900*, and *Glyma.18G022500*. If resistance-type *Rhg1*  $\alpha$ -SNAPs interfere with NSF activities and vesicle trafficking, then the presence of these more canonical wild-type  $\alpha$ -SNAPs is likely to be crucial for the viability of soybeans carrying SCN resistance-conferring haplotypes of *Rhg1*. To determine whether increased levels of wild-type  $\alpha$ -SNAPs could relieve the cytotoxicity of resistance-type *Rhg1*  $\alpha$ -SNAPs, we infiltrated a mixed culture of three parts  $\alpha$ -SNAP<sup>Rhg1</sup>LC to either one part WT- $\alpha$ -SNAP or one part empty vector. Even at this low ratio, coexpression of any of the highly similar Ch<sub>02</sub>, Ch<sub>11</sub>, and Ch<sub>18</sub> soybean  $\alpha$ -SNAPs—but not the divergent Ch<sub>09</sub>  $\alpha$ -SNAP—greatly diminished the cytotoxicity of resistance-type *Rhg1*  $\alpha$ -SNAP (Fig. 3A). Additionally, coexpression of three parts  $\alpha$ -SNAP<sup>Rhg1</sup>LC to one part WT- $\alpha$ -SNAP substantially rescued the exocytosis defect measured using sec-GFP secretion (Fig. 3 B and C). Adjusting the ratio of coinfiltrated  $\alpha$ -SNAP<sup>Rhg1</sup>LC or WT- $\alpha$ -SNAP tipped the cell death vs. tolerance outcome in either direction (Fig. S5C). The above set of experiments suggests that the cell death caused by resistance-type  $\alpha$ -SNAPs in these *N. benthamiana* assays is likely caused by overwhelming the endogenous  $\alpha$ -SNAPs with disruptive *Rhg1*  $\alpha$ -SNAPs.

Having shown that  $\alpha$ -SNAP<sup>Rhg1</sup>WT-L288A or  $\alpha$ -SNAP<sup>Rhg1</sup>WT-L288I expression alone was not cytotoxic in *N. benthamiana*, we tested whether the penultimate leucine is required for wild-type  $\alpha$ -SNAP rescue of cell death from resistance-type  $\alpha$ -SNAPs. As in Fig. 3A, we infiltrated a mixture of three parts  $\alpha$ -SNAP<sup>Rhg1</sup>LC to one part  $\alpha$ -SNAP<sup>Rhg1</sup>WT,  $\alpha$ -SNAP<sup>Rhg1</sup>WT-L288A,  $\alpha$ -SNAP<sup>Rhg1</sup>WT-L288I, or empty vector control. As before, coexpressing  $\alpha$ -SNAP<sup>Rhg1</sup>WT

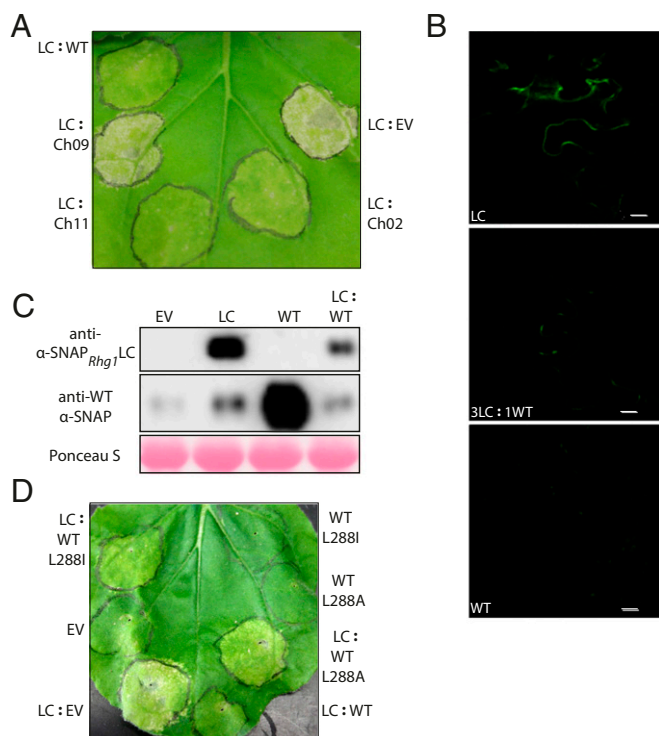


**Fig. 3.** Coexpression of wild-type soybean  $\alpha$ -SNAPs with *Rhg1* resistance-type  $\alpha$ -SNAPs alleviates cell-death symptoms and secretion defects; a penultimate leucine is required. (A) *N. benthamiana* leaves 6 d after agroinfiltration with a 3:1 *Agrobacterium* culture mixture (three parts  $\alpha$ -SNAP<sub>*Rhg1*</sub>LC to one part wild-type soybean  $\alpha$ -SNAP or empty vector control). The soybean wild-type  $\alpha$ -SNAPs are WT ( $\alpha$ -SNAP<sub>*Rhg1*</sub>/WT), *Glyma.18G022500*; Ch<sub>02</sub>, *Glyma.02G260400*; Ch<sub>09</sub>, *Glyma.09G279400*; Ch<sub>11</sub>, *Glyma.11G234500*. (B) Confocal imaging of sec-GFP assays as in Fig. 2C, but including leaves treated with a 3:1 *Agrobacterium* culture mixture as in A. (Scale bars, 20  $\mu$ m.) (C) Immunoblot of leaf samples taken 3 d after agroinfiltration as in A. LC:WT constructs were infiltrated at a 3:1 ratio. (D) Similar to A, with a 3:1 culture mixture of  $\alpha$ -SNAP<sub>*Rhg1*</sub>LC to either  $\alpha$ -SNAP<sub>*Rhg1*</sub>/WT,  $\alpha$ -SNAP<sub>*Rhg1*</sub>/WT with A or I penultimate residue substitutions, or empty vector control.

diminished cytotoxicity. Coexpression of  $\alpha$ -SNAP<sub>*Rhg1*</sub>/WT-L<sub>288A</sub> failed to relieve cell death (Fig. 3D).  $\alpha$ -SNAP<sub>*Rhg1*</sub>/WT-L<sub>288I</sub> coexpression partially decreased cell death compared with empty vector coinfiltration, suggesting that NSF activation may be needed to prevent cell death and that a penultimate isoleucine, but not alanine, may confer partial  $\alpha$ -SNAP function.

#### During *Rhg1*-Mediated SCN Resistance, Resistance-Type $\alpha$ -SNAPs Hyperaccumulate in SCN Feeding Sites and Deplete 20S Complexes.

We previously reported a positive correlation between the copy number of *Rhg1* repeats and higher levels of *Rhg1* transcripts (9). Because high ratios of resistance-type to wild-type  $\alpha$ -SNAPs disrupted trafficking and caused cell death in *N. benthamiana*, we examined whether the balance of wild-type  $\alpha$ -SNAPs to resistance-type  $\alpha$ -SNAPs in soybean normally favors wild-type  $\alpha$ -SNAP activity and is shifted specifically at the nematode feeding site during *Rhg1*-mediated resistance. Roots of non-transgenic soybean cultivar Fayette, which carries high-copy SCN resistance-type *Rhg1*, were inoculated with 200 juvenile SCNs per root or mock-inoculated. Four days later, SCN-infected root regions were isolated and pooled. Endogenous  $\alpha$ -SNAP<sub>*Rhg1*</sub>/HC, WT- $\alpha$ -SNAP, and NSF levels at the developing nematode-induced syncytium were monitored using immunoblots. Substantial increases in  $\alpha$ -SNAP<sub>*Rhg1*</sub>/HC and NSF protein abundance were detected in tissue enriched for SCN syncytia (feeding sites) (Fig. 4A). Moreover, the ratio of  $\alpha$ -SNAP<sub>*Rhg1*</sub>/HC to WT- $\alpha$ -SNAP

in SCN-infested vs. mock-inoculated root regions increased (Fig. 4B). SCN infestation of SCN-susceptible Williams 82 roots did not reveal significant increases in WT- $\alpha$ -SNAP levels in SCN feeding sites compared with mock-inoculated controls (Fig. S10A).

Pooling of SCN-infected root regions includes considerable amounts of nonsyncytial tissue that may dilute detection of stronger responses at infected sites. We therefore used electron microscopy

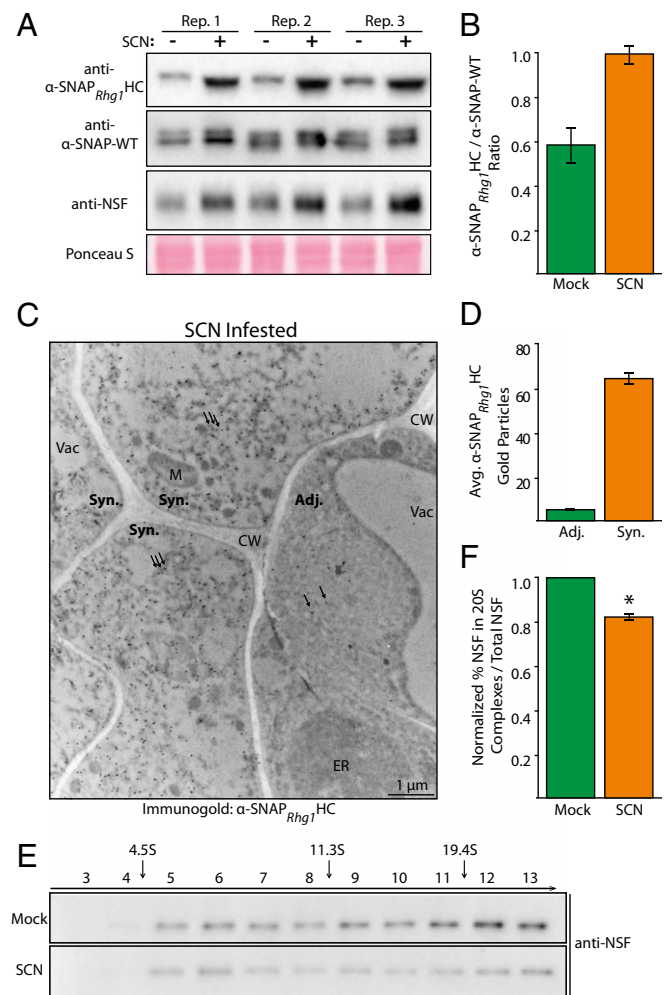


**Fig. 4.**  $\alpha$ -SNAP<sub>*Rhg1*</sub>/HC hyperaccumulates at SCN infection sites in high-copy *Rhg1* soybean accession Fayette and depletes 20S complexes. (A) Immunoblot of tissue samples from SCN-infested root regions harvested 4 d after SCN infection. Blots were probed with the indicated antibodies; quantitative comparisons are valid within rows but not within columns. (B) Densitometric ratio of  $\alpha$ -SNAP<sub>*Rhg1*</sub>/HC to WT  $\alpha$ -SNAPs calculated from the band intensities in A. Error bars show SEM. (C) Brightness-adjusted electron micrograph showing immunogold-labeled  $\alpha$ -SNAP<sub>*Rhg1*</sub>/HC in syncytial cells (Syn.) and adjacent cells (Adj.) 4 d after SCN infection of high-copy *Rhg1* soybean accession Fayette. Arrows highlight 8 of the  $\sim$ 400 immunogold particles in this image. CW, cell wall; M, mitochondrion; Vac, vacuole. (D) Average  $\alpha$ -SNAP<sub>*Rhg1*</sub>/HC immunogold particle counts in syncytial vs. adjacent cells from 30 images across three independent experiments. See Fig. S10 for raw immunogold particle counts, additional images, and antibody specificity controls. Error bars show SEM. (E) Anti-NSF immunoblot of density gradient fractions to detect 20S complexes from SCN-infested Fayette root regions harvested 4 d after SCN infection. (F) Densitometric analysis of NSF from 20S-migrating fractions (fractions 11 to 13) over total NSF (fractions 3 to 13) in SCN-infested root regions. Data from three independent experiments were normalized to 20S NSF abundance from noninfested root regions within each experiment. Paired *t* test, \**P* = 0.022 for similarity to mock. Error bars show SEM.

and immunogold labeling of  $\alpha$ -SNAP<sub>Rhg1</sub>HC to both pinpoint and more accurately assess  $\alpha$ -SNAP<sub>Rhg1</sub>HC protein elevation around the SCN feeding site in soybean cultivar Fayette roots. Immunogold labeling showed hyperaccumulation of the  $\alpha$ -SNAP<sub>Rhg1</sub>HC protein in syncytial cells but not in adjacent nonsyncytial cells (Fig. 4C). Across three independent experiments, ~12-fold more immunogold particles were evident in syncytial cells relative to a similar 2D area of adjacent cells (Fig. 4D and Fig. S10B). Anti- $\alpha$ -SNAP<sub>Rhg1</sub>HC immunogold particles were rare in noninfected samples. Fig. S10 C and D shows images of SCN-infected and noninfected Fayette roots after contrasting, which clarifies cellular organelles but makes immunogold-labeled particles less obvious. To confirm antigen specificity of the anti- $\alpha$ -SNAP<sub>Rhg1</sub>HC antibody in EM/immunogold labeling use, we conducted control experiments in which the antibody was preincubated with a 10-fold molar excess of purified  $\alpha$ -SNAP<sub>Rhg1</sub>HC protein before use on EM sections, and observed no staining in high-copy *Rhg1* roots (Fig. S10E). This indicates strong specificity of the antibody for the intended antigen in EM specimens. No immunogold labeling was observed when only the secondary antibody was used (Fig. S10F). Together, the above results show that *Rhg1*-mediated SCN resistance specifically triggers a shift to increased levels of  $\alpha$ -SNAP<sub>Rhg1</sub>HC in the syncytium.

Because  $\alpha$ -SNAP<sub>Rhg1</sub>HC hyperaccumulates in SCN feeding sites from Fayette, we examined whether 20S complexes are impacted during *Rhg1*-mediated resistance, using density gradient centrifugation as in Fig. 1E. SCN-infested or mock-inoculated root regions from Fayette were isolated and pooled 4 d after inoculation as in Fig. 4A. Densitometric analysis of immunoblots indicated that the proportion of NSF in 20S-migrating fractions is decreased in SCN-infested regions (Fig. 4E and F). We therefore propose that during SCN infection, resistance-type *Rhg1* haplotypes drive a localized hyperaccumulation of defective  $\alpha$ -SNAPs that inhibit NSF function and disrupt normal vesicular trafficking, interfering with pathogen co-option of cellular processes and reducing the viability of the syncytium SCN feeding site.

## Discussion

The present study found that the agriculturally valuable *Rhg1* locus, which combats a highly damaging cyst nematode parasite, encodes disruptive  $\alpha$ -SNAP proteins that impair NSF function.  $\alpha$ -SNAP and NSF are core eukaryotic housekeeping genes that are central to SNARE recycling and vesicle trafficking. Our findings, that C-terminal polymorphisms in resistance-type soybean *Rhg1*  $\alpha$ -SNAPs reduce NSF interaction and 20S stability, disrupt vesicular trafficking, and are cytotoxic, are consistent with animal studies on  $\alpha$ -SNAPs and NSF. In mice,  $\alpha$ -SNAP mutations such as the *hyh* allele are homozygous-lethal, as are NSF-null *comatose* alleles in *Drosophila* (33, 34). Artificial mutations at the penultimate C-terminal leucine of yeast or animal  $\alpha$ -SNAPs no longer stimulate NSF ATPase, impair SNARE recycling, block secretion, and cause apoptosis in cell cultures (14, 25, 29). What is unusual about soybean *Rhg1* is that sabotaging this core housekeeping function contributes to a beneficial trait—a trait that has been widely selected for by soybean breeders in recent decades to help control a disease that annually causes billions of dollars in lost food harvest worldwide.

Resistance through disruption of a core housekeeping process represents a departure from known mechanisms of plant disease resistance (35, 36). Ancient polyploidization in soybean (32) apparently allowed divergence of the *Rhg1*  $\alpha$ -SNAP gene to form an incompletely penetrant dominant-negative allele whose deleterious phenotype is dependent on the relative protein abundance of functional wild-type  $\alpha$ -SNAPs. We provide multiple lines of evidence demonstrating plant disease resistance that is promoted by a dysfunctional variant of an essential gene. Plant resistance to potyviruses is somewhat analogous in that it arises from mutations in the translation initiation factors eIF4G or eIF4E, which are core

housekeeping proteins (37). However, resistance-conferring eIF4 proteins provide a recessive resistance by precluding interactions with the potyvirus VPg, and otherwise appear to retain the normal activities of wild-type eIF4 proteins (37). Resistance to pathogens through compromises in essential gene function, partially analogous to *Rhg1*, has also been reported in humans. For example, resistance to malaria, and possibly typhoid fever, may be enhanced by specific mutations in hemoglobin or cystic fibrosis transmembrane conductance receptor, respectively (38, 39). However, individuals homozygous for these alleles are afflicted with sickle cell anemia or cystic fibrosis. In the case of soybean *Rhg1*, the alleles that confer disease resistance are apparently tolerated because of polyploidization, with the effects of the resistance-conferring dysfunctional  $\alpha$ -SNAPs obscured in most tissues by wild-type  $\alpha$ -SNAP proteins produced by paralogous genes.

The hypothesis that *Rhg1* resistance-type  $\alpha$ -SNAPs interrupt NSF function and vesicle trafficking, yet are tolerated in high-yielding soybean varieties, is strongly supported by our findings that multiple wild-type  $\alpha$ -SNAPs mask the effects of resistance-type  $\alpha$ -SNAPs, even at low doses. It is further supported by the finding that the wild-type-to-resistance-type  $\alpha$ -SNAP ratio shifts during *Rhg1*-mediated SCN resistance, with resistance-type  $\alpha$ -SNAPs hyperaccumulating in the SCN feeding site before its collapse. We do not yet know how the balance in SCN-infected tissues is tipped to an elevated presence of disruptive *Rhg1*  $\alpha$ -SNAP proteins. Elevated *Rhg1* gene expression in syncytia via transcription factor regulation is one obvious hypothesis, but other contributions may come from differential *Rhg1* locus methylation between haplotypes, dynamic infection-associated regulation of *Rhg1* locus methylation, microRNA-mediated transcriptional or posttranscriptional regulation, and syncytium-specific genome endoreduplication (9, 40–42).

A number of recent findings are at least partially consistent with the present finding of disruption of NSF functions and vesicular trafficking by resistance-type *Rhg1*  $\alpha$ -SNAPs. Microarray transcript abundance studies of laser-capture microdissected syncytium samples have indicated that *Rhg1*-mediated disease resistance is accompanied by a cellular stress profile that includes oxidative, cold, osmotic, and unfolded protein stresses (43). Additionally, the high metabolic demands and large-scale membrane reorganizations necessary to form the syncytium (16–18) may amplify cellular sensitivity to noncooperative  $\alpha$ -SNAPs, even in cases where there may be a less significant shift in the ratio of resistance-type *Rhg1*  $\alpha$ -SNAPs to wild-type  $\alpha$ -SNAPs. A study of virulent SCN populations that had recently evolved to reproduce on soybeans carrying high-copy *Rhg1* haplotypes demonstrated allelic imbalance of a SNARE-like effector protein in the nematode (44). Other recent reports suggest that a naturally occurring truncated soybean  $\alpha$ -SNAP enhances SCN resistance through increasing transcription of a Golgi-localized SNARE, syntaxin-31 (45, 46). The amino acid sequence of that truncated  $\alpha$ -SNAP indicates it is encoded by *Glyma.11G234500* on chromosome 11, and hence potential functional overlaps with *Rhg1*-encoded  $\alpha$ -SNAPs on chromosome 18 are unclear (9). Gene silencing of the *Glyma.18G022500* allele that encodes  $\alpha$ -SNAP<sub>Rhg1</sub>HC was previously shown to decrease the SCN resistance of Fayette soybean roots, but statistically significant increases in SCN resistance in SCN-susceptible Williams 82 soybean roots were only observed when  $\alpha$ -SNAP<sub>Rhg1</sub>HC-encoding *Glyma.18G022500* was overexpressed together with the adjacent *Rhg1* genes (8). The mechanisms by which the other *Rhg1*-encoded genes (8), *Glyma.18G022400* and *Glyma.18G022700*, contribute to *Rhg1*-mediated SCN resistance also remain unclear.

In the present study, high levels of *Rhg1* resistance-type  $\alpha$ -SNAPs triggered not only cytotoxicity but also elevated levels of NSF protein. Regulation of NSF activity through post-translational phosphorylation has been reported; however, a cellular feedback mechanism that adjusts NSF levels in response

to  $\alpha$ -SNAP activity is apparently unreported, and may represent a regulatory mechanism present in plants (28). That  $\alpha$ -SNAP<sup>Rhg1</sup> WT-L<sub>288A</sub> did not cause cell death but did elevate NSF levels suggests that this NSF feedback mechanism can, at least in the case of  $\alpha$ -SNAP<sup>Rhg1</sup> WT-L<sub>288A</sub>, compensate for interference with NSF activity. The fact that stimulated increases in NSF abundance did not block the cytotoxicity of the resistance-type  $\alpha$ -SNAP<sup>Rhg1</sup> variants is consistent with the reduced NSF interaction and destabilization of 20S complexes observed for resistance-type  $\alpha$ -SNAPs.

The finding that the more canonical soybean  $\alpha$ -SNAPs counteract the cytotoxicity of resistance-type  $\alpha$ -SNAPs suggests additional areas for study that may provide agriculturally useful findings. For example, it may be functionally relevant that low-copy *Rhg1* soybean haplotypes, which have been more difficult to couple with high grain yields, lack the single wild-type  $\alpha$ -SNAP-encoding *Rhg1* repeat present in high-copy *Rhg1* haplotypes (9). This may make lines carrying the low-copy haplotype more sensitive to negative effects of resistance-type  $\alpha$ -SNAPs. As another matter, the  $\alpha$ -SNAP<sup>Rhg1</sup>LC<sub>splice</sub> protein encoded by low-copy *Rhg1* was not observed to accumulate. Up-regulation of the proportion of alternatively spliced  $\alpha$ -SNAP<sup>Rhg1</sup>LC transcript could provide a bypass that reduces disruptive  $\alpha$ -SNAP production and promotes balance with regard to wild-type  $\alpha$ -SNAPs. Other areas for future work are suggested by the positive correlation between the strength of SCN resistance and copy number of high-copy ( $\alpha$ -SNAP<sup>Rhg1</sup>HC-encoding) *Rhg1* repeats (9, 21, 47, 48). Improved SCN resistance may be obtained if haplotypes can be identified or generated that carry more *Rhg1* copies than the current mainstay 10-copy haplotype. With transgene or CRISPR-Cas9 technologies, it may be possible to more directly boost *Rhg1* effectiveness based on our findings regarding higher doses of resistance-type  $\alpha$ -SNAPs or substitutions at the penultimate  $\alpha$ -SNAP residue. Extensive screens of soybean accessions carrying low-copy  $\alpha$ -SNAP<sup>Rhg1</sup>LC-encoding *Rhg1* haplotypes (21) have detected *Rhg1* copy numbers only at or below three. This suggests that with this more strongly cytotoxic  $\alpha$ -SNAP there may be a need to limit *Rhg1* copy number to balance SCN resistance functions against the requirement for most tissues to contain a low relative dosage of dysfunctional  $\alpha$ -SNAPs to obtain healthy high-yielding soybean lines. It may be possible, however, to overcome this limitation by achieving more pronounced up-regulation of resistance-type  $\alpha$ -SNAP abundance at sites of SCN infection. More generally, the paradigm of disease resistance through high local expression of a toxic variant of a core housekeeping protein may be applicable to other host–pathogen interactions.

## Materials and Methods

**Recombinant Protein Production and in Vitro  $\alpha$ -SNAP/NSF Binding Assays.** NSF and  $\alpha$ -SNAP were expressed from pRham N-His SUMO (Lucigen) in *Escherichia coli* and purified, and the epitope tag was removed before binding experiments according to the manufacturer's instructions. In vitro NSF binding assays were performed with immobilized  $\alpha$ -SNAP essentially as in refs. 10 and 25 and quantified using ImageJ (49). Further details are in *SI Materials and Methods*.

**Oligonucleotides Used.** The oligonucleotides used are listed in *Table S1*.

**Transient *Agrobacterium*-Mediated Protein Expression in *N. benthamiana*.** *Agrobacterium tumefaciens* strain GV3101 (pMP90) cultures were syringe-infiltrated at OD<sub>600</sub> 0.60 (unless otherwise noted) into leaves of 4-wk-old *N. benthamiana* plants, similar to ref. 50. Expression of  $\alpha$ -SNAP or NSF was performed with the previously described binary vector pSM101 with the soybean ubiquitin promoter or pGWB vectors with the 35S promoter. All *N. benthamiana* cytotoxicity assays were conducted on at least three different leaves on each date and repeated on at least two separate dates with similar results.

**Glycerol Gradient Ultracentrifugation and Fractionation.** Glycerol gradient ultracentrifugation and fractionation to detect 20S complexes were performed similar to refs. 51 and 52 and quantified using ImageJ. Solubilized membrane proteins were separated in a gradient buffer nonpermissive to ATP hydrolysis. Fraction sedimentation was monitored by parallel cofractionation of protein standards.

**Transgenic Soybean Root Production.** Transgenic soybean roots were generated by transformation of soybean with *Agrobacterium rhizogenes* strain Arqua1 as described in ref. 8.

**Antibodies, Immunoblots, and Coimmunoprecipitation.** Affinity-purified polyclonal antibodies were raised against synthetic peptide sequences matching different  $\alpha$ -SNAP C termini or soybean NSF<sub>CHO7</sub> (New England Peptide or Pacific Immunology). Antibody specificity was validated through immunoblots on tissue lysates and recombinant proteins (Fig. S2). Immunoblotting and co-IP analysis was performed as in ref. 50.

Detailed information regarding recombinant protein production, binding assays, 20S complex analyses, protein expression in *N. benthamiana* leaves, sec-GFP and Syp61-mCherry confocal microscopy, immunodetection, electron microscopy, and other experimental procedures is provided in *SI Materials and Methods*.

**ACKNOWLEDGMENTS.** We thank Dr. Sebastian Bednarek for sharing recombinant mammalian NSF<sub>CHO</sub> proteins and substantial guidance, as well as Dr. Declan James and Dr. Marisa Otegui for suggestions. We also thank Dr. Roger Innes (Indiana University) for sharing the Syp61-mCherry construct, Dr. Hugo Zheng (McGill University) for providing the sec-GFP construct, and Amy Yan for assistance with plant cultivation. This work was funded primarily by U.S. Department of Agriculture-National Institute of Food and Agriculture-Agriculture and Food Research Initiative Award 2014-67013-21775 (to A.F.B.), and also by the United Soybean Board and Wisconsin Soybean Marketing Board. This material is based upon work supported by the National Science Foundation Graduate Research Fellowship Program under Grant DGE-1256259 (to A.M.B.).

- Jahn R, Scheller RH (2006) SNAREs—Engines for membrane fusion. *Nat Rev Mol Cell Biol* 7(9):631–643.
- Wickner W, Schekman R (2008) Membrane fusion. *Nat Struct Mol Biol* 15(7):658–664.
- Inada N, Ueda T (2014) Membrane trafficking pathways and their roles in plant-microbe interactions. *Plant Cell Physiol* 55(4):672–686.
- Collins NC, et al. (2003) SNARE-protein-mediated disease resistance at the plant cell wall. *Nature* 425(6961):973–977.
- Asrat S, de Jesús DA, Hempstead AD, Ramabhadran V, Isberg RR (2014) Bacterial pathogen manipulation of host membrane trafficking. *Annu Rev Cell Dev Biol* 30:79–109.
- Uemura T, et al. (2012) Qa-SNAREs localized to the trans-Golgi network regulate multiple transport pathways and extracellular disease resistance in plants. *Proc Natl Acad Sci USA* 109(5):1784–1789.
- Hoefle C, Hückelshoven R (2008) Enemy at the gates: Traffic at the plant cell pathogen interface. *Cell Microbiol* 10(12):2400–2407.
- Cook DE, et al. (2012) Copy number variation of multiple genes at Rhg1 mediates nematode resistance in soybean. *Science* 338(6111):1206–1209.
- Cook DE, et al. (2014) Distinct copy number, coding sequence, and locus methylation patterns underlie Rhg1-mediated soybean resistance to soybean cyst nematode. *Plant Physiol* 165(2):630–647.
- Barnard RJ, Morgan A, Burgoyne RD (1997) Stimulation of NSF ATPase activity by alpha-SNAP is required for SNARE complex disassembly and exocytosis. *J Cell Biol* 139(4):875–883.
- Vivona S, et al. (2013) Disassembly of all SNARE complexes by N-ethylmaleimide-sensitive factor (NSF) is initiated by a conserved 1:1 interaction between  $\alpha$ -soluble NSF attachment protein (SNAP) and SNARE complex. *J Biol Chem* 288(34):24984–24991.
- Zhao M, et al. (2015) Mechanistic insights into the recycling machine of the SNARE complex. *Nature* 518(7537):61–67.
- Ryu JK, et al. (2015) Spring-loaded unraveling of a single SNARE complex by NSF in one round of ATP turnover. *Science* 347(6229):1485–1489.
- Zick M, Orr A, Schwartz ML, Merz AJ, Wickner WT (2015) Sec17 can trigger fusion of trans-SNARE paired membranes without Sec18. *Proc Natl Acad Sci USA* 112(18):E2290–E2297.
- Gheysen G, Mitchum MG (2011) How nematodes manipulate plant development pathways for infection. *Curr Opin Plant Biol* 14(4):415–421.
- Niblack TL, Lambert KN, Tylka GL (2006) A model plant pathogen from the kingdom Animalia: *Heterodera glycines*, the soybean cyst nematode. *Annu Rev Phytopathol* 44:283–303.
- Davis EL, Hussey RS, Mitchum MG, Baum TJ (2008) Parasitism proteins in nematode-plant interactions. *Curr Opin Plant Biol* 11(4):360–366.
- Kyndt T, Vieira P, Gheysen G, de Almeida-Engler J (2013) Nematode feeding sites: Unique organs in plant roots. *Planta* 238(5):807–818.
- Donald PA, et al. (2006) Assessing *Heterodera glycines*-resistant and susceptible cultivar yield response. *J Nematol* 38(1):76–82.
- Concibido VC, Diers BW, Arelli PR (2004) A decade of QTL mapping for cyst nematode resistance in soybean. *Crop Sci* 44(4):1121–1131.

21. Lee TG, Kumar I, Diers BW, Hudson ME (2015) Evolution and selection of Rhg1, a copy-number variant nematode-resistance locus. *Mol Ecol* 24(8):1774–1791.
22. Colgrove AL, Niblack TL (2008) Correlation of female indices from virulence assays on inbred lines and field populations of *Heterodera glycines*. *J Nematol* 40(1):39–45.
23. Niblack T, Colgrove A, Colgrove K, Bond J (January 18, 2008) Shift in virulence of soybean cyst nematode is associated with use of resistance from PI 88788. *Plant Health Prog*, 10.1094/PHP-2008-0118-01-RS.
24. Lambert KN, et al. (2005) Selection of *Heterodera glycines* chorismate mutase-1 alleles on nematode-resistant soybean. *Mol Plant Microbe Interact* 18(6):593–601.
25. Barnard RJ, Morgan A, Burgoyne RD (1996) Domains of alpha-SNAP required for the stimulation of exocytosis and for *N*-ethylmaleimide-sensitive fusion protein (NSF) binding and activation. *Mol Biol Cell* 7(5):693–701.
26. Dalal S, Rosser MF, Cyr DM, Hanson PI (2004) Distinct roles for the AAA ATPases NSF and p97 in the secretory pathway. *Mol Biol Cell* 15(2):637–648.
27. Barszczewski M, et al. (2008) A novel site of action for alpha-SNAP in the SNARE conformational cycle controlling membrane fusion. *Mol Biol Cell* 19(3):776–784.
28. Zhao C, Slevin JT, Whiteheart SW (2007) Cellular functions of NSF: Not just SNAPs and SNAREs. *FEBS Lett* 581(11):2140–2149.
29. Naydenov NG, et al. (2012) Loss of soluble *N*-ethylmaleimide-sensitive factor attachment protein  $\alpha$  ( $\alpha$ SNAP) induces epithelial cell apoptosis via down-regulation of Bcl-2 expression and disruption of the Golgi. *J Biol Chem* 287(8):5928–5941.
30. Batoko H, Zheng HQ, Hawes C, Moore I (2000) A Rab1 GTPase is required for transport between the endoplasmic reticulum and Golgi apparatus and for normal Golgi movement in plants. *Plant Cell* 12(11):2201–2218.
31. Gu Y, Innes RW (2011) The KEEP ON GOING protein of *Arabidopsis* recruits the ENHANCED DISEASE RESISTANCE1 protein to *trans*-Golgi network/early endosome vesicles. *Plant Physiol* 155(4):1827–1838.
32. Schmutz J, et al. (2010) Genome sequence of the palaeopolyploid soybean. *Nature* 463(7278):178–183.
33. Chae TH, Kim S, Marz KE, Hanson PI, Walsh CA (2004) The *hyh* mutation uncovers roles for alphaSnap in apical protein localization and control of neural cell fate. *Nat Genet* 36(3):264–270.
34. Sanyal S, Krishnan KS (2001) Lethal comatose mutation in *Drosophila* reveals possible role for NSF in neurogenesis. *Neuroreport* 12(7):1363–1366.
35. Dangl JL, Horvath DM, Staskawicz BJ (2013) Pivoting the plant immune system from dissection to deployment. *Science* 341(6147):746–751.
36. Niks RE, Qi X, Marcel TC (2015) Quantitative resistance to biotrophic filamentous plant pathogens: Concepts, misconceptions, and mechanisms. *Annu Rev Phytopathol* 53:445–470.
37. Kang BC, Yeam I, Jahn MM (2005) Genetics of plant virus resistance. *Annu Rev Phytopathol* 43:581–621.
38. Pier GB, et al. (1998) *Salmonella typhi* uses CFTR to enter intestinal epithelial cells. *Nature* 393(6680):79–82.
39. Elguero E, et al. (2015) Malaria continues to select for sickle cell trait in Central Africa. *Proc Natl Acad Sci USA* 112(22):7051–7054.
40. de Almeida Engler J, Gheysen G (2013) Nematode-induced endoreduplication in plant host cells: Why and how? *Mol Plant Microbe Interact* 26(1):17–24.
41. Song QX, et al. (2011) Identification of miRNAs and their target genes in developing soybean seeds by deep sequencing. *BMC Plant Biol* 11:5.
42. Yu A, et al. (2013) Dynamics and biological relevance of DNA demethylation in *Arabidopsis* antibacterial defense. *Proc Natl Acad Sci USA* 110(6):2389–2394.
43. Kandath PK, et al. (2011) The soybean Rhg1 locus for resistance to the soybean cyst nematode *Heterodera glycines* regulates the expression of a large number of stress- and defense-related genes in degenerating feeding cells. *Plant Physiol* 155(4):1960–1975.
44. Bekal S, et al. (2015) A SNARE-like protein and biotin are implicated in soybean cyst nematode virulence. *PLoS One* 10(12):e0145601.
45. Matsye PD, et al. (2012) The expression of a naturally occurring, truncated allele of an  $\alpha$ -SNAP gene suppresses plant parasitic nematode infection. *Plant Mol Biol* 80(2):131–155.
46. Pant SR, Krishnavajhala A, McNeece BT, Lawrence GW, Klink VP (2015) The syntaxin 31-induced gene, LESION SIMULATING DISEASE1 (LSD1), functions in *Glycine max* defense to the root parasite *Heterodera glycines*. *Plant Signal Behav* 10(1):e977737.
47. Yu N, Lee TG, Rosa DP, Hudson M, Diers BW (August 31, 2016) Impact of Rhg1 copy number, type, and interaction with Rhg4 on resistance to *Heterodera glycines* in soybean. *Theor Appl Genet*, 10.1007/s00122-016-2779-y.
48. Lee TG, Diers BW, Hudson ME (June 16, 2016) An efficient method for measuring copy number variation applied to improvement of nematode resistance in soybean. *Plant J* 10.1111/tpj.13240.
49. Schindelin J, et al. (2012) Fiji: An open-source platform for biological-image analysis. *Nat Methods* 9(7):676–682.
50. Song J, Keppler BD, Wise RR, Bent AF (2015) PARP2 is the predominant poly(ADP-ribose) polymerase in *Arabidopsis* DNA damage and immune responses. *PLoS Genet* 11(5):e1005200.
51. Bassham DC, Raikhel NV (1999) The pre-vacuolar t-SNARE AtPEP12p forms a 20S complex that dissociates in the presence of ATP. *Plant J* 19(5):599–603.
52. Rancour DM, Dickey CE, Park S, Bednarek SY (2002) Characterization of AtCDC48. Evidence for multiple membrane fusion mechanisms at the plane of cell division in plants. *Plant Physiol* 130(3):1241–1253.
53. Klock HE, Lesley SA (2009) The polymerase incomplete primer extension (PIPE) method applied to high-throughput cloning and site-directed mutagenesis. *Methods Mol Biol* 498:91–103.
54. Hanson PI, Roth R, Morisaki H, Jahn R, Heuser JE (1997) Structure and conformational changes in NSF and its membrane receptor complexes visualized by quick-freeze/deep-etch electron microscopy. *Cell* 90(3):523–535.
55. Crooks GE, Hon G, Chandonia JM, Brenner SE (2004) WebLogo: A sequence logo generator. *Genome Res* 14(6):1188–1190.

# Supporting Information

Bayless et al. 10.1073/pnas.1610150113

## SI Materials and Methods

**Recombinant Proteins.** ORFs for all *Rhg1*  $\alpha$ -SNAPs and soybean NSF, *Glyma.07G195900* and *Glyma.13G180100*, were cloned into the expression vector pRham N-His-SUMO Kan according to the manufacturer's guidelines (Lucigen). Recombinant  $\alpha$ -SNAP<sub>*Rhg1*</sub>WT with the final 10 C-terminal residues truncated [ $\alpha$ -SNAP<sub>*Rhg1*</sub>WT(-10)] was generated from the pRham N-His-SUMO  $\alpha$ -SNAP<sub>*Rhg1*</sub>WT vector using the polymerase incomplete primer extension (PIPE) mutagenesis method (53) to remove the final 10 codons. All expression constructs were chemically transformed into the expression strain "E. cloni 10G" (Lucigen), grown to OD<sub>600</sub> 0.60, and then induced with 0.2% L-rhamnose (Sigma) for ~8 h at 37 °C or overnight at 28 °C. Notably, recombinant production of the  $\alpha$ -SNAP<sub>*Rhg1*</sub>LC<sup>Splice</sup> protein required stringent expression conditions (induced at 18 °C for ~10 h) compared with the other  $\alpha$ -SNAPs to recover any soluble protein. Purified recombinant mammalian His-NSF was a kind gift of Sebastian Bednarek (University of Wisconsin–Madison). Soluble, native recombinant His-SUMO- $\alpha$ -SNAPs or His-SUMO-NSF proteins were purified with PerfectPro Ni-NTA resin (5 PRIME), with similar procedures as described in ref. 54, although no subsequent gel filtration steps were performed. Following the elution of the His-SUMO–fusion proteins, overnight dialysis was performed at 4 °C in 20 mM Tris (pH 8.0), 150 mM NaCl, 10% (vol/vol) glycerol, and 1.5 mM Tris-(2-carboxyethyl)phosphine. The His-SUMO affinity/solubility tags were cleaved from  $\alpha$ -SNAP or soybean NSF using 1 or 2 units of SUMO Express protease (Lucigen) and separated by rebinding of the tag with Ni-NTA resin and collecting the recombinant protein from the flowthrough. Recombinant protein purity was assessed by Coomassie blue staining and quantified via a spectrophotometer.

**In Vitro  $\alpha$ -SNAP and NSF Binding Assays.** In vitro NSF binding assays were performed essentially as outlined in refs. 10 and 25. Briefly, 20  $\mu$ g of each recombinant  $\alpha$ -SNAP protein was placed in a 1.5-mL polypropylene tube and incubated at room temperature for 20 min. Unbound  $\alpha$ -SNAP was washed with SNAP wash buffer [25 mM Tris, pH 7.4, 50 mM KCl, 1 mM DTT, 1 mg/mL bovine serum albumin (BSA)], and 20  $\mu$ g of recombinant NSF was added and incubated on ice for 10 min. The NSF in solution was then removed and each sample was washed twice to remove unbound NSF. Samples were then boiled in 1 $\times$  SDS loading buffer, separated by 8% SDS/PAGE, and silver-stained using the ProteoSilver Kit (Sigma-Aldrich) following the manufacturer's guidelines. The amount of NSF bound to various  $\alpha$ -SNAPs was calculated by densitometric analysis with ImageJ.

**Plasmid Constructs.** Transient overexpression of soybean  $\alpha$ -SNAPs or soybean NSF was performed using the previously described soybean ubiquitin promoter in the binary vector pSM101 (8) or with the 35S promoter from pGWB6 (50). The soybean  $\alpha$ -SNAP ORFs for *Glyma.18G022500*, *Glyma.11G234500*, *Glyma.02G260400*, and *Glyma.09G279400* and the soybean NSF ORFs for *Glyma.07G195900* and *Glyma.13G180100* were PCR-amplified from Williams 82, Fayette, or Forrest cDNAs generated using the iScript cDNA Synthesis Kit (Bio-Rad) and KAPA HiFi polymerase (Kapa Biosystems). Each respective ORF was placed directly under the control of the soybean ubiquitin promoter in the vector pBlue-Script using the polymerase incomplete primer extension (PIPE) method (53) and sequence-verified.  $\alpha$ -SNAP or NSF expression cassettes were digested with XbaI/PstI or SbfI/AvrII (New England Biolabs) and gel-extracted using the QIAquick Gel Extraction Kit (Qiagen). Purified DNA fragments were then ligated into the binary

vector pSM101 using T4 DNA ligase (New England Biolabs). Mutagenesis of  $\alpha$ -SNAPs to create penultimate residue substitutions, C-terminal truncations, or ATPase-null NSF constructs was also performed using PIPE-based mutagenesis with KAPA HiFi polymerase.

**Transient *Agrobacterium* Expression in *Nicotiana benthamiana*.** *Agrobacterium tumefaciens* strain GV3101 (pMP 90) containing specified expression constructs was syringe-infiltrated at OD<sub>600</sub> 0.60 (unless otherwise noted) into young leaves of ~4-wk-old *N. benthamiana* plants. All GV3101 cultures were grown overnight at 28 °C in 25  $\mu$ g mL<sup>-1</sup> kanamycin and rifampicin and induced for ~2.5 h in 10 mM Mes (pH 5.60), 10 mM MgCl<sub>2</sub>, and 100  $\mu$ M acetosyringone before leaf infiltration. *N. benthamiana* plants were grown at 25 °C with a photoperiod of 16 h light at 100  $\mu$ E·m<sup>-2</sup>·s<sup>-1</sup> and 8 h dark. For  $\alpha$ -SNAP<sub>*Rhg1*</sub>LC complementation with WT  $\alpha$ -SNAP coinfiltration, three volumes of  $\alpha$ -SNAP<sub>*Rhg1*</sub>LC at OD<sub>600</sub> 0.60 were well-mixed with one volume of the specified WT  $\alpha$ -SNAP at OD<sub>600</sub> 0.60 or empty vector at OD<sub>600</sub> 0.60 immediately before coinfiltration. For sec-GFP coexpression experiments, sec-GFP was coinfiltrated at OD<sub>600</sub> 0.015 with a specified *Rhg1*  $\alpha$ -SNAP at OD<sub>600</sub> 0.60 or empty vector at OD<sub>600</sub> 0.60 (30). For co-IP analysis, soybean NSF<sub>Ch07</sub>-HA cultures were mixed with either GFP- $\alpha$ -SNAP<sub>*Rhg1*</sub>HC or GFP- $\alpha$ -SNAP<sub>*Rhg1*</sub>WT and coinfiltrated at OD<sub>600</sub> 0.40 for each construct.

**Coimmunoprecipitation.** cDNAs of NSF<sub>Ch07</sub> and  $\alpha$ -SNAP<sub>*Rhg1*</sub>HC or  $\alpha$ -SNAP<sub>*Rhg1*</sub>WT were cloned into the HA-tagged pSM101 (soybean ubiquitin promoter) and GFP-tagged pGWB6 (35S promoter) vectors, respectively, and transformed into *A. tumefaciens* GV3101 (pMP90). Leaves of 4-wk-old *N. benthamiana* plants were agroinfiltrated at OD<sub>600</sub> 0.4, and leaf tissues were harvested 3 d later. Total proteins were extracted in lysis buffer [50 mM Tris-HCl, pH 7.5, 150 mM NaCl, 5 mM EDTA, 0.2% Triton X-100, 10% (vol/vol) glycerol, plant protease inhibitor mixture (Sigma) at 1:100]. Immunoprecipitation was carried out as described (50) with anti-GFP (Abcam) antibody at 4 °C overnight followed by incubation with protein A beads (Thermo Scientific) for 1 to 2 h. The beads were washed three times with extraction buffer without protease inhibitors. The precipitated proteins were eluted with 1 $\times$  SDS loading buffer, subjected to SDS/PAGE, immunoblotted with anti-HA (Roche) and anti-GFP (Clontech) antibodies, and detected using SuperSignal West Pico or Dura chemiluminescent substrate (Thermo Scientific). Immunoprecipitation with transgenic soybean roots of high-copy *Rhg1* variety Fayette expressing NSF<sub>Ch07</sub>-HA was performed similarly, except that pull-down was performed with anti-HA antibody (Roche) and detection was performed with the custom  $\alpha$ -SNAP antibodies described below.

**Glycerol Gradient Ultracentrifugation and Fractionation.** Glycerol gradient ultracentrifugation was performed similar to refs. 51 and 52. 20S complex abundance was quantified as the amount of NSF in ~20S-migrating complexes over the total amount of NSF present, and was calculated by densitometric analysis of NSF band intensity using ImageJ (49). Gradients of 40 to 17.5% (vol/vol) glycerol were layered into 13  $\times$  51-mm Ultra-Clear tubes (Beckman Coulter) and allowed to settle at 4 °C for 1 h before use. Transgenic *N. benthamiana* leaves were harvested at 3 d post infiltration. SCN-infested or mock-inoculated Fayette soybean roots were harvested at 4 d post infection. *N. benthamiana* leaf lysates or lysates from pooled soybean root regions were prepared as outlined for *Arabidopsis* roots in ref. 51, and membrane pellets were detergent-solubilized in a

gradient buffer nonpermissive to ATP hydrolysis (20 mM Hepes, pH 7.50, 50 mM KCl, 2 mM EDTA, 2 mM DTT, 1 mM ATP, 1% Triton X-100). Equal amounts of solubilized membrane proteins, as determined by Bradford assay, were then layered onto the gradients and separated by centrifugation at  $125,000 \times g$  for 18 h in an MLS-50 swinging bucket rotor (Beckman Coulter). Four-hundred-microliter fractions were collected from the top, except for the final 100- $\mu$ L fractions, which included pellet material and were excluded from final analyses. Fraction sedimentation was monitored by parallel cofractionation of protein standards of known sedimentation: BSA (4.4S), alcohol dehydrogenase (7.6S), catalase (11.3S), and thyroglobulin (19.4S) (Fig. S4).

**Antibody Production.** Affinity-purified polyclonal antibodies were raised against synthetic peptide sequences matching the final six or seven C-terminal  $\alpha$ -SNAP residues: "EEDDLT," "EQHEAIT," or "EEYEVIT" for wild-type, high-, or low-copy  $\alpha$ -SNAPs, respectively. For soybean NSF, a synthetic peptide, "ETEKNVRDLFADAEQDQRTRGDESD," matching residues 300 to 324, was used. Resistance-type  $\alpha$ -SNAP peptides and antibodies were produced by New England Peptide, whereas NSF and wild-type  $\alpha$ -SNAP antibodies were produced by Pacific Immunology. Antibody specificity was validated through immunoblots using various recombinantly produced  $\alpha$ -SNAP and NSF proteins and also root lysates of high- or low-copy *Rhg1*-containing lines, transgenic *N. benthamiana* leaves expressing various  $\alpha$ -SNAPs, or Williams 82 (single-copy) hairy roots expressing various  $\alpha$ -SNAPs (Fig. S2).

**Immunoblots.** Soybean roots or *N. benthamiana* leaf tissue was flash-frozen in liquid nitrogen and homogenized in 50 mM Tris-HCl (pH 7.5), 150 mM NaCl, 5 mM EDTA, 0.2% Triton X-100, 10% (vol/vol) glycerol, and protease inhibitor mixture in a PowerLyzer 24 (MO BIO) for three cycles at 15 s each, with flash freezing in-between cycles. Bradford assays were performed on each sample, and the same amount of total protein was loaded in each sample lane for SDS/PAGE. Immunoblots for either *Rhg1*  $\alpha$ -SNAP were incubated overnight at 4 °C in 5% (wt/vol) nonfat dry milk TBS-T (50 mM Tris, 150 mM NaCl, 0.05% Tween 20) at 1:1,000. NSF immunoblots were performed similarly, except incubations were for 1 h at room temperature. Secondary horseradish peroxidase-conjugated goat anti-rabbit IgG was added at 1:10,000 and incubated for 1 h at room temperature on a platform shaker, followed by four washes with TBS-T. Chemiluminescence detection was performed with SuperSignal West Pico or Dura chemiluminescent substrate (Thermo Scientific) and developed using a ChemiDoc MP chemiluminescent imager (Bio-Rad).

**Transgenic Soybean Hairy Root Production.** Transgenic soybean hairy roots were generated by transformation of soybean with *Agrobacterium rhizogenes* strain Arqua1 as described (8).

**Confocal Microscopy.** Live-cell imaging experiments were performed using an inverted laser-scanning confocal microscope (ELYRA LSM 780; Carl Zeiss) with a 20 $\times$  or 40 $\times$  water-immersion objective. Transformed leaves were analyzed 72 h after infiltration. The excitation wavelength for GFP was 488 nm and the emitted fluorescence was collected with a 510–525-nm emission filter. Individual experiments for sec-GFP fluorescence were performed by single-imaging frame collection using identical laser output levels and imaging conditions on cells expressing sec-GFP or coexpressed with empty vector or the indicated soybean SNAPs. Images were captured using a standardized scan area of  $442.2 \times 442.2 \mu\text{m}$  (pixel size 0.87  $\mu\text{m}$ ), with a frame size of  $512 \times 512$  and a scan time of 968.14 ms. The 488-nm laser intensity was set at 2.5, with a master gain setting of 725 and a pinhole of 32.3 (0.84 airy units). At least 25 images were taken for each expression construct. Sec-GFP fluorescence was quantified using Fiji software (49). GFP fluorescence intensity was calculated by highlighting each image with the Rectangular Selection tool and analyzing for mean pixel intensity of the total epidermal cell-surface area ( $\mu\text{m}^2$ ). Syp61-mCherry imaging was performed similarly, except image collection was performed with a 40 $\times$  wet mount on mesophyll cells. The excitation wavelength for mCherry was 561 nm. Four separate plants from three independent experiments were used, and >50 images of each treatment were collected.

**Electron Microscopy.** Syncytia from soybean roots (Fayette) inoculated with 200 juvenile stage 2 (J2) SCNs (Race 0) were hand-sectioned with a razor at 4 days post infection. Root sections were fixed in 0.1% glutaraldehyde and 4% (vol/vol) paraformaldehyde in 0.1 M sodium phosphate buffer (PB) (pH 7.4) overnight (under vacuum for the first hour). Samples were washed four times with 0.1 M PB, dehydrated in ethanol, and embedded in LR White. Ultrathin sections (~90-nm) were taken using an ultramicrotome (UC-6; Leica) and mounted on nickel slot grids. For the immunogold labeling procedure, grids were incubated on drops of 50 mM glycine/PBS for 15 min followed by drops of prepared blocking buffer (Aurion) for 30 min and then equilibrated in 0.1% BSA-C/PBS (incubation buffer) (Aurion). Next, grids were incubated with the indicated antibodies diluted 1:200 (in incubation buffer) overnight at 4 °C, washed five times in incubation buffer, and incubated for 2 h with goat anti-rabbit antibody conjugated to 15-nm gold (Aurion) diluted 1:25 in incubation buffer. After six washes in incubation buffer and two 5-min washes in PBS, the grids were fixed for 5 min in 2.0% (vol/vol) glutaraldehyde in 0.1 M phosphate buffer, followed by two 5-min washes in 0.1 M phosphate buffer and five 2-min washes in water. Finally, the grids were contrasted with 2% (vol/vol) aqueous uranyl acetate and Reynolds lead citrate. Images were collected with a MegaView III digital camera on a Philips CM120 transmission electron microscope.

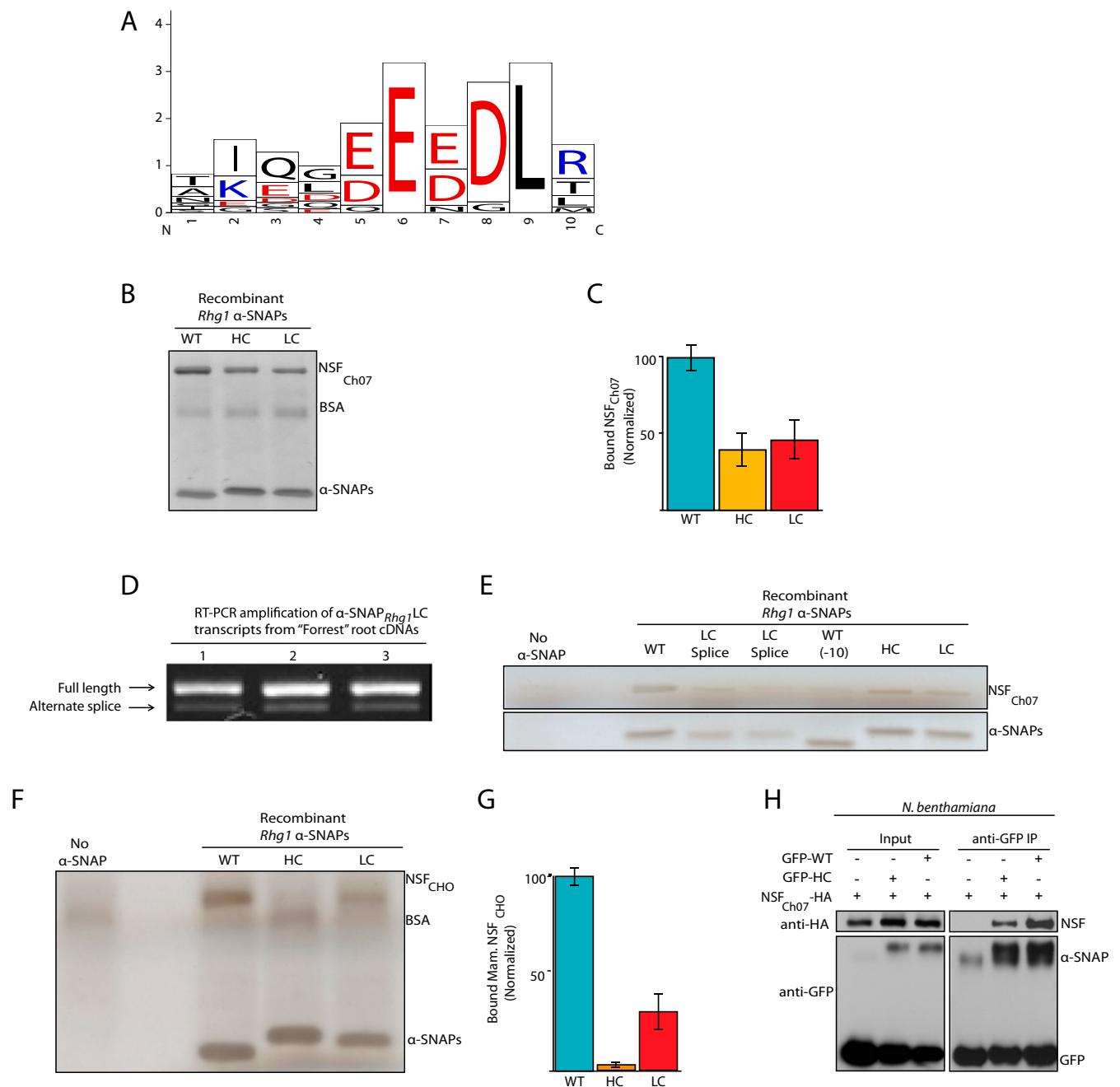


**Fig. S1.**  $\alpha$ -SNAP extreme C terminus is highly conserved among eukaryotes and critical for NSF binding. (A) Logo showing conservation of the final 10 C-terminal  $\alpha$ -SNAP residues from model organisms across diverse phyla, similar to ref. 9.  $\alpha$ -SNAP C-terminal consensus was generated from the following species: *Chlamydomonas reinhardtii*, *Saccharomyces cerevisiae*, *Physcomitrella patens*, *Arabidopsis thaliana*, *Medicago truncatula*, *Nicotiana tabacum*, *Caenorhabditis elegans*, *Drosophila melanogaster*, *Danio rerio*, *Xenopus laevis*, *Gallus gallus*, *Rattus norvegicus*, and *Homo sapiens*. The conservation logo was generated using WebLogo (55). (B) Silver-stained SDS/PAGE of recombinant soybean NSF<sub>Ch07</sub> bound in vitro by recombinant wild-type (WT), low-copy (LC), or high-copy (HC) *Rhg1*  $\alpha$ -SNAP proteins. (C) Densitometric quantification of NSF<sub>Ch07</sub> bound by *Rhg1*  $\alpha$ -SNAPs as in Fig. 1C; data are from four independent NSF<sub>Ch07</sub> experiments. Error bars show SEM. (D) Agarose gel showing RT-PCR product generated due to the presence of both full-length transcript and the alternate splice product. RT-PCR was performed on low-copy *Rhg1* line Forrest cDNA with a primer directly upstream of the splice site and at a sequence unique to the low-copy *Rhg1*  $\alpha$ -SNAP C terminus. Alternate splicing represents roughly 20% of total low-copy  $\alpha$ -SNAP transcripts. (E) Silver-stained SDS/PAGE of recombinant soybean NSF<sub>Ch07</sub> bound to recombinant *Rhg1*  $\alpha$ -SNAPs, including the alternately spliced low-copy  $\alpha$ -SNAP protein (LC<sub>splice</sub>) or a 10-residue C-terminal truncation of  $\alpha$ -SNAP<sub>*Rhg1*WT</sub> [WT(-10)]. (F) As in B, but with a *Rhg1*-encoded  $\alpha$ -SNAP binding assay with recombinant Chinese hamster ovary NSF (NSF<sub>CHO</sub>). (G) Densitometric analysis of in vitro NSF<sub>CHO</sub> binding from four independent experiments. Error bars show SEM. (H) NSF coimmunoprecipitation upon anti-GFP immunoprecipitation (IP) of GFP- $\alpha$ -SNAP<sub>*Rhg1*WT</sub> or GFP- $\alpha$ -SNAP<sub>*Rhg1*HC</sub> coexpressed with soybean NSF<sub>Ch07</sub>-HA in *N. benthamiana* leaves. Input: total protein samples before immunoprecipitation.

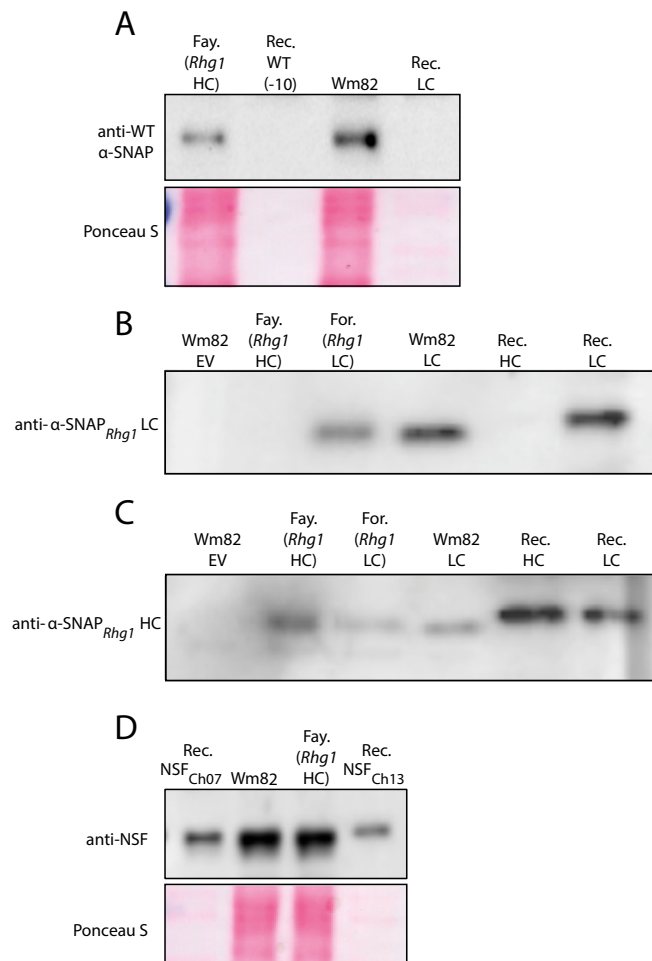


**Fig. S2.** Confirming the specificity of custom-generated  $\alpha$ -SNAP and NSF antibodies. (A) Immunoblot test of anti- $\alpha$ -SNAP WT on root lysates from Fayette (Fay.) or Williams 82 (Wm82), recombinant WT  $\alpha$ -SNAP truncated at the final 10 C-terminal residues and thereby lacking the epitope region [Rec. WT(-10)], or recombinant  $\alpha$ -SNAP<sub>*Rhg1*</sub>LC protein (Rec. LC). Note:  $\alpha$ -SNAP WT antibody was raised to the highly conserved  $\alpha$ -SNAP C terminus and is thus cross-reactive with most WT  $\alpha$ -SNAPs. (B) Immunoblot test of anti- $\alpha$ -SNAP<sub>*Rhg1*</sub>LC (low-copy) on root lysates from Fayette (endogenous high-copy *Rhg1*), Forrest (endogenous low-copy *Rhg1*), or transgenic Williams 82 (single-copy *Rhg1*) roots expressing  $\alpha$ -SNAP<sub>*Rhg1*</sub>LC or an empty vector control (EV), or purified recombinant  $\alpha$ -SNAP<sub>*Rhg1*</sub>LC or recombinant  $\alpha$ -SNAP<sub>*Rhg1*</sub>HC protein. (C) Similar to B, but an immunoblot test of anti- $\alpha$ -SNAP<sub>*Rhg1*</sub>HC (high-copy). Note:  $\alpha$ -SNAP<sub>*Rhg1*</sub>HC antibody is cross-reactive with  $\alpha$ -SNAP<sub>*Rhg1*</sub>LC but not with WT  $\alpha$ -SNAPs. (D) Immunoblot test of anti-NSF on recombinant NSF<sub>Ch07</sub> or NSF<sub>Ch13</sub> or root lysates from Fayette or Williams 82. As expected, the anti-soybean NSF antibody is also cross-reactive with the *N. benthamiana* NSF protein (e.g., Fig. 2).

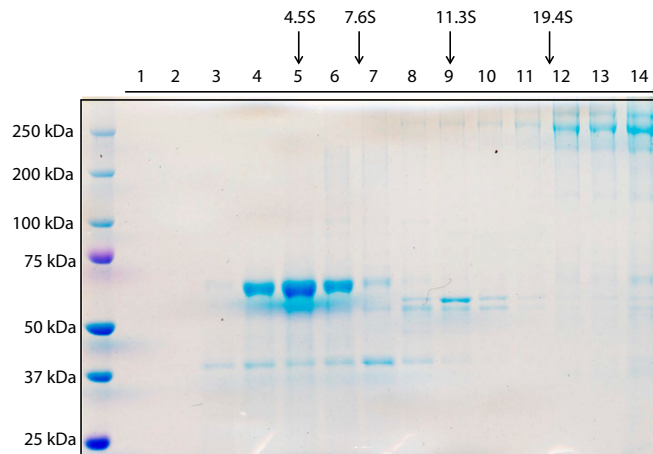


**Fig. S3.** Density gradient fractionation of protein standards of known sedimentation, performed in the same run as one of the fractionations that detected the presence of NSF in 20S complexes (e.g., Fig. 1G). Sedimentation was performed similar to refs. 51 and 52. Protein standards were detected by SDS/PAGE and Coomassie blue stain. Protein standards used were thyroglobulin (19.4S), ~250-kDa dimer; catalase (11.3S), ~60-kDa tetramer; yeast alcohol dehydrogenase (7.6S), ~37-kDa tetramer; and BSA (4.5S), ~65 kDa.

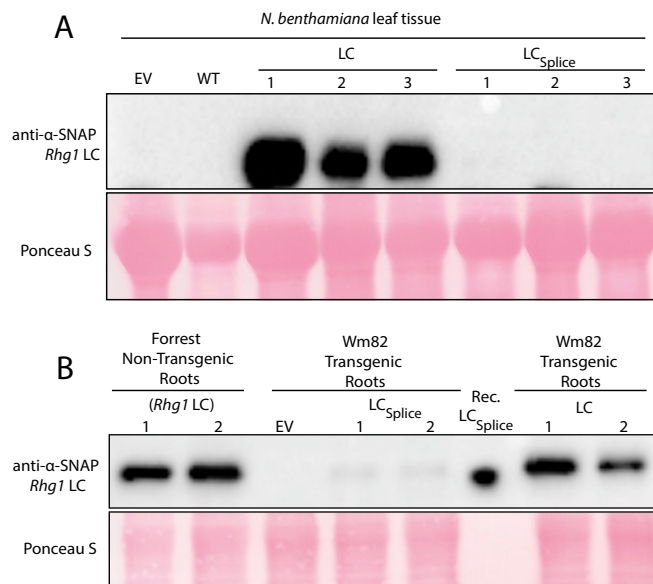


**Fig. S4.**  $\alpha$ -SNAP protein encoded by alternate splicing of the low-copy  $\alpha$ -SNAP transcript does not appreciably accumulate in soybean roots or *N. benthamiana* leaves. (A) Anti- $\alpha$ -SNAP<sub>Rhg1LC</sub> immunoblot of three separate samples of agroinfiltrated *N. benthamiana* leaves expressing  $\alpha$ -SNAP WT,  $\alpha$ -SNAP<sub>Rhg1LC</sub>,  $\alpha$ -SNAP<sub>Rhg1LC\_Splice</sub>, or empty vector. Ponceau S staining shows relative protein levels. Immunoblot labels: EV, empty vector; LC,  $\alpha$ -SNAP<sub>Rhg1LC</sub>; LC<sub>Splice</sub>,  $\alpha$ -SNAP<sub>Rhg1LC\_Splice</sub>; WT,  $\alpha$ -SNAP<sub>Rhg1</sub> WT. (B) Anti- $\alpha$ -SNAP<sub>Rhg1LC</sub> immunoblot of soybean Forrest root lysates, transgenic root lysates from Williams 82 expressing  $\alpha$ -SNAP<sub>Rhg1LC</sub>, empty vector, or  $\alpha$ -SNAP<sub>Rhg1LC\_Splice</sub>, or purified recombinant  $\alpha$ -SNAP<sub>Rhg1LC\_Splice</sub> to confirm anti- $\alpha$ -SNAP<sub>Rhg1LC</sub> recognition of the  $\alpha$ -SNAP<sub>Rhg1LC\_Splice</sub> protein. Note that a low-abundance band is present in Wm82 transgenic roots agroinfiltrated with  $\alpha$ -SNAP<sub>Rhg1LC\_Splice</sub> construct but not empty vector.

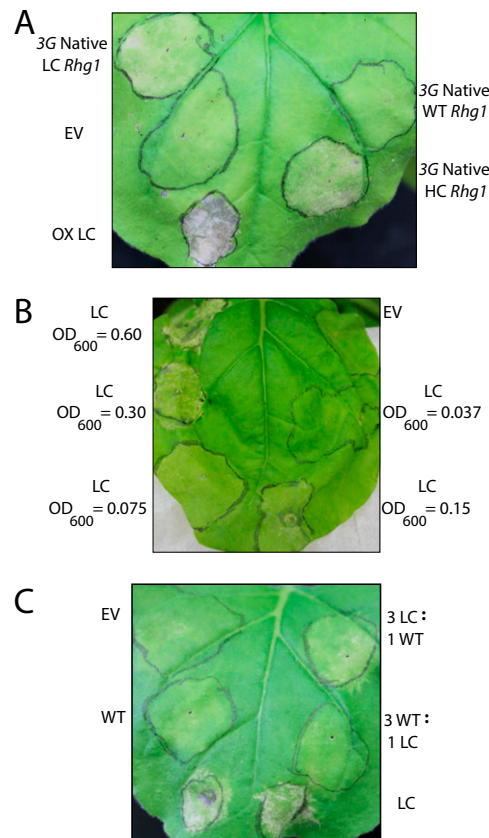


**Fig. 55.** *Rhg1* resistance-type  $\alpha$ -SNAP cytotoxicity is dosage-dependent and occurs independent of the other *Rhg1* locus-encoded genes. (A) *N. benthamiana* leaf agroinfiltrated with native genomic *Rhg1* three-gene blocks (3G Native *Rhg1*) containing *Glyma.18G022400* or *Glyma.18G022700* and the *Glyma.18G022500* alleles encoding the respective single-copy, low-copy, or high-copy *Rhg1*  $\alpha$ -SNAPs. Overexpressed  $\alpha$ -SNAP<sub>*Rhg1*</sub>LC (OX LC) and an empty vector were agroinfiltrated as controls. Cytotoxic symptoms in *N. benthamiana* still occur from expression of  $\alpha$ -SNAPs driven by native soybean *Rhg1* promoters, albeit at a decreased rate and severity compared with expression from a strong ubiquitin promoter. All constructs were infiltrated at OD<sub>600</sub> 0.60. An image is shown for 9 d after agroinfiltration. LC,  $\alpha$ -SNAP<sub>*Rhg1*</sub>LC expressed from the soybean ubiquitin promoter. (B) *N. benthamiana* leaf agroinfiltrated with serial twofold dilutions of  $\alpha$ -SNAP<sub>*Rhg1*</sub>LC or an empty vector control. Leaf shown 6 d after agroinfiltration. (C) *N. benthamiana* leaf agroinfiltrated with a 1:3 vs. a 3:1 mixture of  $\alpha$ -SNAP<sub>*Rhg1*</sub>LC and  $\alpha$ -SNAP<sub>*Rhg1*</sub>WT shows further decreases in cytotoxic progression compared with  $\alpha$ -SNAP<sub>*Rhg1*</sub>LC alone. Leaf shown ~8 d after infiltration.

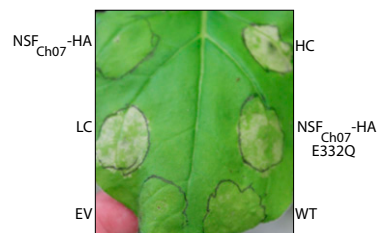


**Fig. 56.** Expression of an NSF lacking ATPase activity phenocopies  $\alpha$ -SNAP *Rhg1* expression and is cytotoxic to *N. benthamiana*. *N. benthamiana* leaf expressing soybean NSF<sub>Ch07</sub>-HA, the ATPase-null NSF<sub>Ch07</sub>-HA (E<sub>332</sub>Q),  $\alpha$ -SNAP<sub>*Rhg1*</sub>LC,  $\alpha$ -SNAP<sub>*Rhg1*</sub>HC,  $\alpha$ -SNAP<sub>*Rhg1*</sub>WT, or empty vector control at 7 d after agroinfiltration. HC,  $\alpha$ -SNAP<sub>*Rhg1*</sub>HC. NSF and  $\alpha$ -SNAP expression was from the soybean ubiquitin promoter. NSF-HA<sub>Ch07</sub>E<sub>332</sub>Q but not WT NSF<sub>Ch07</sub>-HA expression causes cell death similar to  $\alpha$ -SNAP<sub>*Rhg1*</sub>LC or HC.

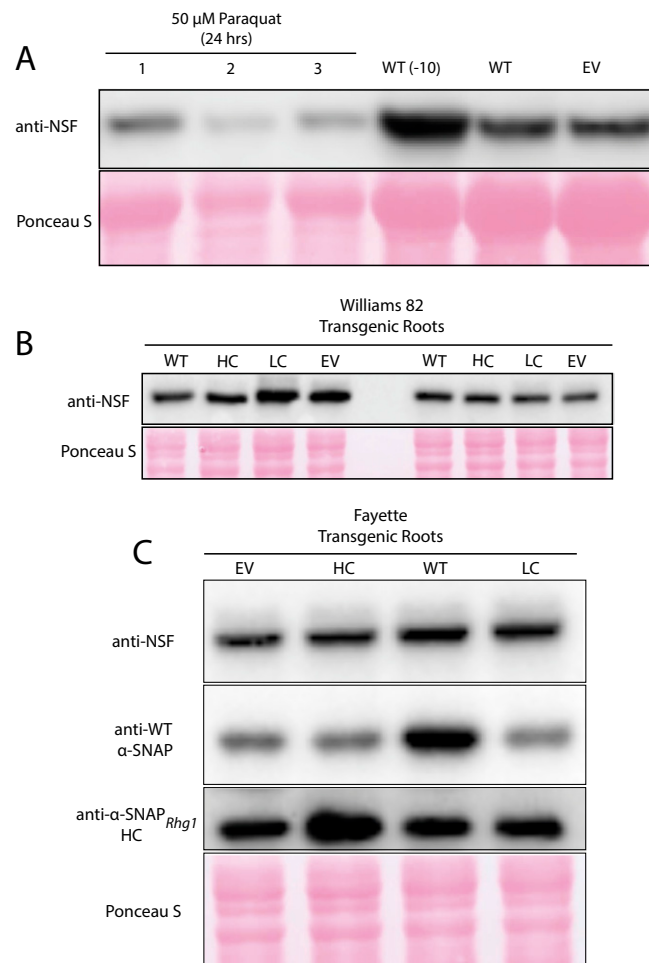


**Fig. S7.** Expression of  $\alpha$ -SNAP<sub>Rhg1</sub>/WT(-10) raises NSF levels in *N. benthamiana* leaves, but paraquat treatment of *N. benthamiana* leaves, or transgenic expression of *Rhg1* resistance-type  $\alpha$ -SNAP in soybean hairy roots, does not detectably raise abundance of NSF. (A) Immunoblot of *N. benthamiana* leaf lysates 24 h after infiltrating with 50  $\mu$ M paraquat (methyl viologen) or 3 d after agroinfiltration delivery of the indicated  $\alpha$ -SNAPs. (B) Anti-NSF immunoblots on transgenic Williams 82 root lysates expressing the indicated  $\alpha$ -SNAPs. (C) Anti-NSF immunoblots on transgenic Fayette root lysates expressing the respective  $\alpha$ -SNAPs. Ponceau S staining shows relative protein levels. WT(-10),  $\alpha$ -SNAP<sub>Rhg1</sub>/WT(-10).

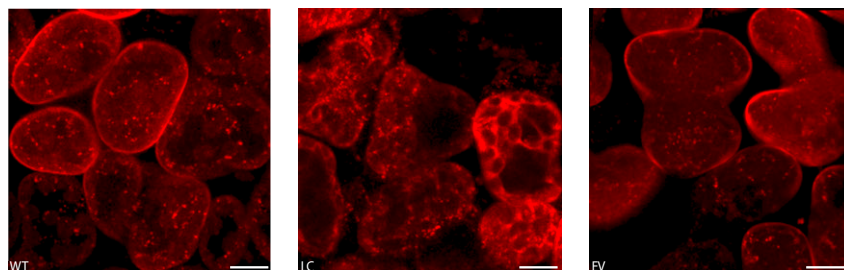


**Fig. S8.** Resistance-type  $\alpha$ -SNAP expression appears to disrupt localization of the *trans*-Golgi network/early endosome marker Syp61-mCherry in *N. benthamiana*. Confocal images of *N. benthamiana* mesophyll cells coexpressing Syp61-mCherry and  $\alpha$ -SNAP<sub>Rhg1</sub>/WT,  $\alpha$ -SNAP<sub>Rhg1</sub>/LC, or empty vector. Images are at 3 d after agroinfiltration;  $n = 20$  for each construct. (Scale bars, 20  $\mu$ m.)



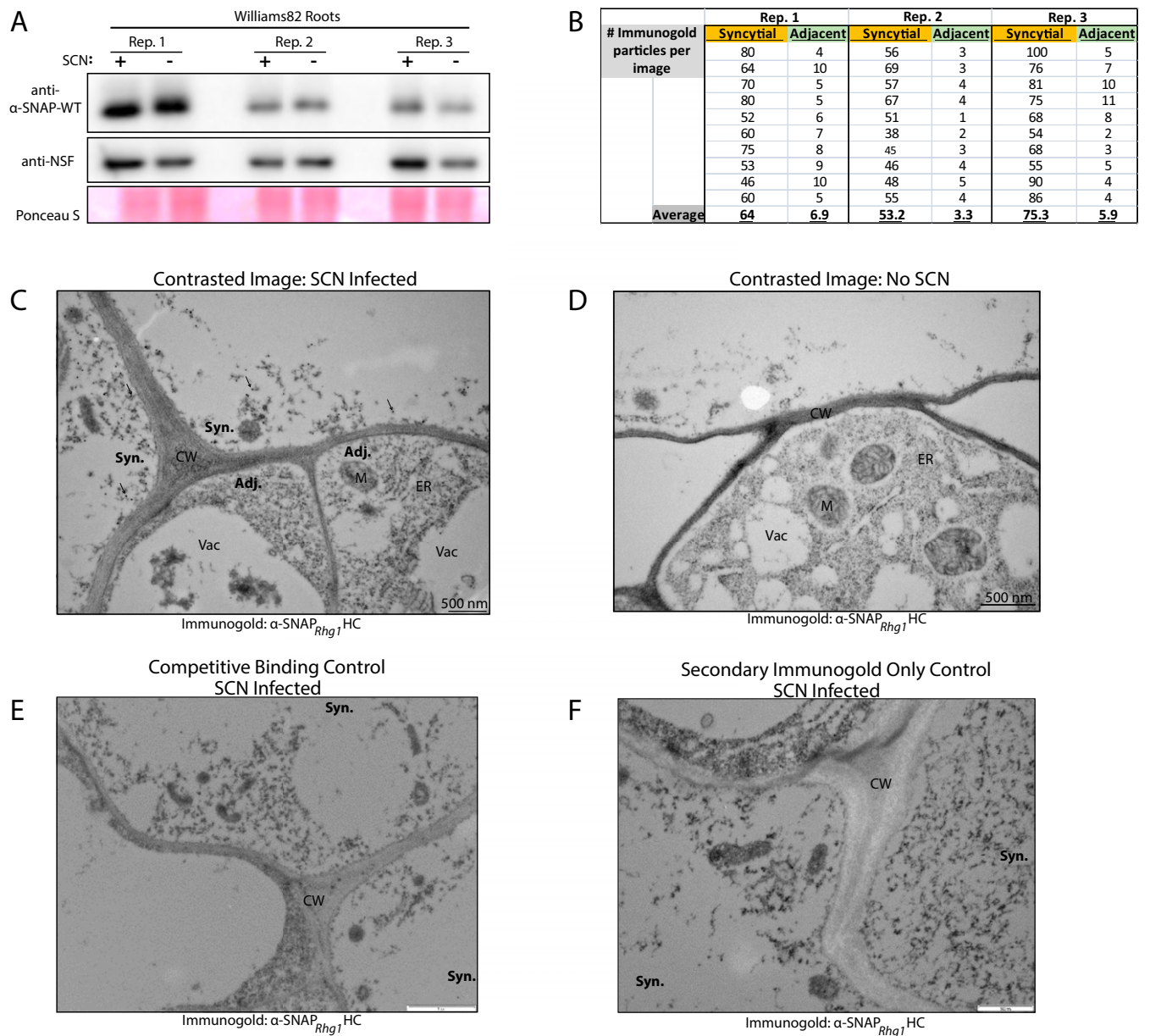


**Fig. S10.** Quantification of *Rhg1*  $\alpha$ -SNAPs in developing syncytia and confirmation of  $\alpha$ -SNAP<sub>*Rhg1*</sub>HC specificity when used in immunogold labeling of electron microscopy sections of SCN-infested roots. (A) Immunoblot of Williams 82 tissue samples from SCN-infested root regions harvested 4 d after SCN infection. Blots were probed with the indicated antibodies. (B) Number of  $\alpha$ -SNAP<sub>*Rhg1*</sub>HC immunogold particles detected in syncytial cells vs. adjacent cells in SCN-infested Fayette roots. Data from three independent experiments are shown. (C) Contrasted electron micrograph of the syncytium and adjacent cell of Fayette root infested with SCNs, after immunogold label detection using anti- $\alpha$ -SNAP<sub>*Rhg1*</sub>HC primary antibody [similar to Fig. 4C (noncontrasted)]. Adj., adjacent cell; CW, cell wall; ER, endoplasmic reticulum; M, mitochondrion; Syn., syncytial cell; Vac, vacuole. Arrows highlight four of many gold particle-labeled  $\alpha$ -SNAP<sub>*Rhg1*</sub>HC regions. (D) Contrasted electron micrograph of mock-inoculated Fayette root after immunogold label detection using anti- $\alpha$ -SNAP<sub>*Rhg1*</sub>HC primary antibody. (E) Electron micrograph of a syncytium site of Fayette root infested with SCNs, where the primary anti- $\alpha$ -SNAP<sub>*Rhg1*</sub>HC antibody was competitively bound with a 10-fold molar excess of antigen (recombinant  $\alpha$ -SNAP<sub>*Rhg1*</sub>HC protein) before immunolabeling of the microscopy section. After the initial competitive binding, anti- $\alpha$ -SNAP<sub>*Rhg1*</sub>HC primary antibody was incubated with fixed cross-sections of SCN-infested Fayette roots and probed with secondary goat anti-rabbit antibody conjugated to 15-nm gold particles. Multiple cross-sections were examined using competitively bound  $\alpha$ -SNAP<sub>*Rhg1*</sub>HC primary antibody and little to no gold particle labeling was observed, indicating high antigen specificity. (F) Immunogold labeling using only secondary goat anti-rabbit antibody on SCN-infested roots. No previous incubations with  $\alpha$ -SNAP<sub>*Rhg1*</sub>HC antibody were performed. Little to no gold particle labeling is present, indicating  $\alpha$ -SNAP<sub>*Rhg1*</sub>HC labeling in SCN-infested roots is highly specific. (Scale bars in E and F, 1  $\mu$ m.)

**Table S1. Oligonucleotides used**

Name	Sequence, 5'-3'
SuNSF 7 Rev	GTGGCGGCCGCTCTATTATAACCTAACCAACATCCTGGAGGCAATCATA
ExpV For	TAA TAG AGC GGC CGC CAC C
SuNSF 13 Rev	GTGGCGGCCGCTCTATTATCTAACACATCCTGGAGGCAATCATAG
SuNSF 7 For	CGC GAA CAG ATT GGA GGT GCG AGT CGG TTC GGG TTA TC
SuNSF 13 For	CGCGAACAGATTGGAGGTTTCGGCTTATCGTCTTCGCTCTTCCTC
ExpV Rev	ACC TCC AAT CTG TTC GCG GTG
NSF 07g SUMO Exp For	CGC GAA CAG ATT GGA GGTGCGAGTCGGTTCGGGTATC
NSF 07g SUMO Exp Rev	gtggcgccgctctattaTAACCTAACCAACATCCTGGAGGCAATCATG
NSF 13 cDNA spec Rev	GGTCATTACAGTTTGAGAGCAGCAC
NSF 13 cDNA spec For	GCCAAGAAACAGAGAAACATAGAGGC
NSF 07 E332Q For	cAAATTGATGCTATTTGCAAGTCAAGAGGTTC
NSF 07 E332Q Rev	CATCTCGAGTTGAACCTCTTGACTTG
NSF 07g cDNA For	ATG GCG AGT CGG TTC GGG TTA TCG T
NSF 07g cDNA Rev	TAA CCT AAC AAC ATC CTG GAG GCA ATC ATA GAA ATG AGC
NSF 07g SUMO Exp For	CGC GAA CAG ATT GGA GGTGCGAGTCGGTTCGGGTATC
NSF 07g SUMO Exp Rev	gtggcgccgctctattaTAACCTAACCAACATCCTGGAGGCAATCAT
pRham 2590 Fuse Will Rev	GTGGCGGCCGCTCTATTAAGTAAGATCATCCTCCTCAAGTCTTTGG
pRham 2590 Fuse For	CGCGAACAGATTGGAGGTGCCGATCAGTTATCGAAGGGA GAG G
pRham 2590 Fuse Pek Rev	gtggcgccgctctattaagtaataacctcactcctcaagttccttgg
WT aSNAP C-10 Trunc Rev	tcaTTTCAGCTTTTCCTTACCCTTAAGAGa
WT aSNAP C-10 Trunc For	GAAAAGCTGAAATGatGAATTGTACCTTTAATATTCCTGGTGGTTGG
Ch 09 aSNAP cDNA For	GTGTTGGCAAAGGGTGATGAC
Ch 09 aSNAP cDNA Rev	CAAAGCTGAGAGTAACCTTAATTGGCAG
Ch 02 aSNAP CDNA For	TTCCAATATGGGCGATCATTGG
Ch 02 aSNAP CDNA Rev	ACCGAAAGAAGACCATGGTGC
Ch 11 aSNAP CDNA For	CGATCAATCCATCCATCTTCACTTGC
Ch 11 aSNAP CDNA Rev	CAAACAATAGGTCCAACCGCCAG
Ch 11 aSNAP PIPE Rev	AATTCGCCCTTTTCAAGTAAGATCATCCTCCTCAAGTCTTTGG
Ch 11 aSNAP PIPE For	TTGTTGACTCGACAGATGGCCGATCAGTTATCCAAAGG
Ch 09 aSNAP PIPE For	ttgTTGACTCGACAGATGCTTGTGCCCTTGTTTCG
Ch 09 aSNAP PIPE Rev	AATTCGCCCTTTTTCATGTCAAATCATCATCTTCCATCTCTTTTAC
Ch 02 aSNAP PIPE For	TTGTTGACTCGACAGATGGCCGATCATTGGCCAG
Ch 02 aSNAP PIPE Rev	AATTCGCCCTTTTCAAGTAAGATCATCCTCCTCGATTCTTTTG
pBS ter PIPE For	TGAAAAGGGCGAATTCGACCC
pBS Gmubi PIPE Rev	CTGTGAGTCAACAATCACAGATAAATC
For aSNAP HC PIPE, 289 Ala	GCT GCT ACT TGA TAA TAG AGC GGC CGC CA
Rev aSNAP HC PIPE, 289 Leu	AGT AAG AGC CTC ATG CTG CTC AAG TTC TTT GGC
For aSNAP HC PIPE, 289 Leu	TGAGCAGCATGAGGCTCTTACTTGAACCCAGCTTTCTT GTA CAA AG
Rev aSNAP HC PIPE, 289 ala	AGT AGC AGC CTC ATG CTG CTC AAG TTC TTT GGC
For aSNAP WT PIPE, L288A	TGAGGAGGATGATGCTACTTGAACCCAGCTTTCTTGTA CAA AG
Rev aSNAP WT PIPE, L288A	AGT AGC ATC ATC CTC CTC AAG TTC TTT GGC
Rev aSNAP WT PIPE, L288I	AGT AAT ATC ATC CTC CTC AAG TTC TTT GGC
aSNAP Rhg1 LC	ctctgtaaagaggaggttggtgctat
aSNAP Rhg1 LC Rev qPCR	gcaatgtccgccaacaatc
aSNAP Rhg1 LC Splice	gtaaagaggaggaactggatcc
aSNAP LC cDNA Rev	AGTAATAACCTCATACTCCTCAAGTT
WT aSNAP cDNA Rev	AGTAAGATCATCCTCCTCAAGTCT
SUMO aSNAP WT Rev	tcaTTTCAGCTTTTCCTTACCCTTAAGAGa
SUMO aSNAP WT C-10 Trunc For	gaaaagctgaaatgatgaattgtacctttaaattcctggtggttgg
pRham aSNAP WT Rev	gtg gcg gcc gct cta tta agt aag atc atc ctc ctc aag ttc ttt gg
pRham aSNAP For	cgc gaa cag att gga ggt gcc gat cag tta tcg aag gga gag g
pRham 2590 Fuse Peking Rev	gtg gcg gcc gct cta tta agt aat aac ctc ata ctc ctc aag ttc ttt gg
pRham 2590 Fuse Fay Rev	gtg gcg gcc gct cta tta agt aat agc ctc atg ctg ctc aag ttc

For, forward; qPCR, quantitative PCR; Rev, reverse.